# RESULTS
# &
# DISCUSSION

# RESULTS & DISCUSSION

## FUNCTIONAL ANTAGONISM ASSAY: PRELIMINARY STUDIES

### *Establishing baseline values for agonists and studies with standard antagonists of $\alpha_1$ and angII receptor*

The primary aim of the studies was to identify a potential candidate that showed balanced modulation of the $\alpha_1$ and the angII receptors. This was brought about by studying the antagonistic ability of different test compounds against phenylephrine and angII mediated contractions of the rat thoracic aorta. Similar studies were also performed with the standard compounds for the purpose of direct comparison. The studies were initiated with the evaluation of prazosin against phenylephrine mediated contractions. Receptor classification study was not performed since it has been very well reported that rat aorta expresses adrenoceptors of the $\alpha_{1D}$ type (Kenny *et al*, 1995; Deng *et al*, 1996; Stassen *et al*, 1997). Phenylephrine initiated contractions in the rat aortic strips at concentrations ranging from 15 nM or higher. It was observed that addition of 1μM prazosin caused a rightward parallel shift in the concentration-response-curve of phenylephrine (Figure 7). $pA_2$ calculations revealed a value of 8.08 ± 0.11 which was less than that reported in the available literature (Hussain & Marshall, 1997 [9.9]; Yamamoto & Koike, 2001 [9.65]). Higher (10μM) or lower (0.1μM) concentrations of prazosin did not induce significant changes in the $pA_2$ values. Hence, this value was considered as the standard value in all further studies and reported accordingly. It is known that prazosin is a specific $\alpha_1$-receptor (subtype non-specific) antagonist. Prazosin mediates antagonism of specific and non-specific $\alpha_1$-receptor agonists in different tissues like aorta (Stassen *et al*, 1997), vas deferens (Ohmura *et al*, 1992), anococcygeus muscle (Adenekan and Tayo, 1982), mesenteric arteries (Yamamoto and Koike, 2001), brain (Wee *et al*, 2008) and in different cell-types expressing the $\alpha_1$-receptor subtypes. This study allowed establishment of baseline values for phenylephrine and simultaneously permitted calculation of $pA_2$ value of prazosin.

Similar studies were performed on separate set of aortic strips using angiotensin II as the agonist where losartan was used as the standard antagonist. Concentration Response Curve (CRC) was obtained with angII at concentrations ranging from 10 nM

and higher. Incubation of losartan (0.1μM) or higher concentrations (≤ 10μM) resulted in a rightward parallel shift of the CRC of angII (Figure 8) with $pA_2$ value being 8.43 ± 0.21.

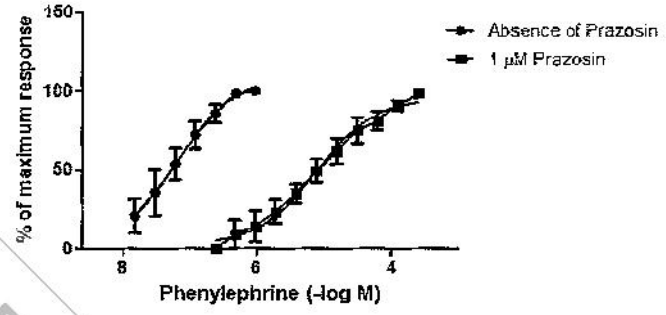


Figure 7: Concentratation response curves of phenylephrine in presence and absence of prazosin.

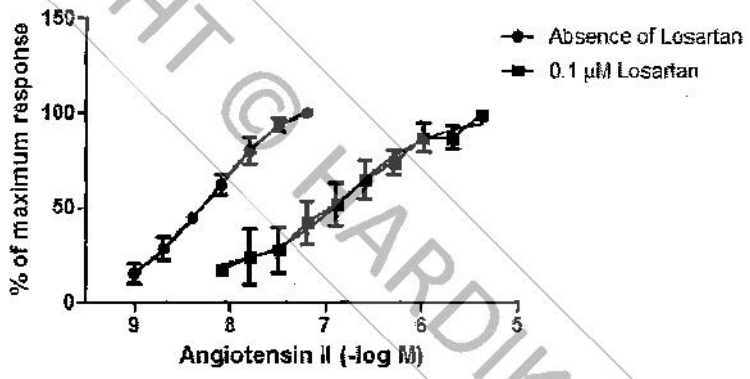


Figure 8: Concentration response curves to angiotensin II in presence and absence losartan.

Several studies have previously reported the $pA_2$ value of losartan and the results of the present study are in agreement with those studies (Rossi *et al*, 2006; Rossi *et al*, 2007; Laneri *et al*, 2011). Losartan, a non-peptide angII antagonist, is known to inhibit angII receptor activation by binding to it in a reversible manner (Johnston, 1995). Losartan mediated antagonism of angII receptor mediated effects has been shown in brain, hepatic, renal, pulmonary and arterial tissues (Guimaraes *et al*, 1998).

Since standard antagonists for both the receptors in question showed a rightward parallel shift in the CRC of their respective agonists and the antagonism mediated by them was found to be surmountable at higher concentrations of the agonist, it was

assumed that this method was suitable for studying the competitive antagonists of $\alpha_1$ and angII receptors.

***Cross screening of standard compounds on the $\alpha_1$ and the angII receptors***

A wide variety of chemical structures possess $\alpha_1$-adrenoceptor blocking activity (Jain *et al*, 2008). Similar observations have been made for angII receptor antagonists (Naik *et al*, 2010). After studying the structure activity relationships of both the classes of drugs minutely it became evident that the drug binding sites of both the receptors could accommodate wide structural variations in the active molecules and if that presumption was correct, then designing of dual acting $\alpha_1$ and angII antagonists should not be an unachievable task. Prazosin, the prototypical $\alpha_1$ blocker was chosen as the

responses (Tables 7-12). These results forced us to have a relook at the mechanism of antihypertensive actions of both prazosin and losartan. When neutral molecules without any characteristic side chains could show dual $\alpha_1$- and angII-receptor antagonism, was it possible for prazosin and losartan also to show dual antagonism at both the receptors? $pA_2$ value determinations of both of the standard lead molecules confirmed the correctness of our assumption of wide structural tolerance by both the receptors in their active spaces - prazosin exhibited potent dual antagonism at $\alpha_1$- ($pA_2$ 8.08±0.11) as well as angII receptors ($pA_2$ 8.26±0.10) while losartan was found to be a potent antagonist at angII-receptor ($pA_2$ 8.43±0.21) but a poor ($pA_2$ 5.46±0.41) on eat $\alpha_1$-receptor when evaluated on rat aortic strip using phenylephrine and angII as agonists. Other compounds were also screened and it was found that while doxazosin and terazosin also mediated angII receptor antagonism ($pA_2$ 6.61 ± 0.4 and 6.39 ± 0.4 for doxazosin and terazosin, respectively) albeit only moderately, $\alpha_1$-receptor antagonism potential was practically absent in valsartan and olmesartan ($pA_2$ values could not be calculated). In all these cases the slopes of the CRCs were not very different from unity (Figures 9 & 10).

This was a totally surprising finding unreported in the literature. It may be because prazosin possessed some stereochemical features required to bind to the $AT_1$ receptor or may possess some three dimensional features required to fill in $AT_1$ receptor pockets. Postural hypotension is one of the common side effects of $\alpha_1$ receptor blockers frequently reported by patients. Prazosin, being the most prominent in this regard, causes orthostatic hypotension in majority of the patients (Take *et al*, 1998; Rieckert, 1996). Based on our findings, we take the liberty to suggest that prazosin mediates fall in blood pressure through blockade of not only $\alpha_1$-receptors but $AT_1$ receptor as well. An absence of baroreceptor mediated reflex in patients receiving prazosin therapy is responsible for orthostatic hypotension (Gupta & Lipsitz, 2007). The baroreceptor reflex is regulated through the sympathetic as well as the parasympathetic nervous system. An activation of the SNS results in a consequential release of norepinephrine (Rowell, 1993). The primary action of norepinephrine released in this manner is to increase the resistance of blood vessels, ultimately maintaining the blood pressure. Secondly, the released norepinephrine also stimulates the secretion of rennin (Takagi *et al*, 1992) and ultimately, formation of angII. This *de novo* formation of angII can cause direct vasoconstriction mediated through $AT_1$ receptors. But as per our findings,

prazosin blocks this arm through competitive blockade of $AT_1$ receptors. As a novel finding, we can therefore assume, that potency of $\alpha_1$-blockers is, additionally a function of $AT_1$ receptor antagonism also.

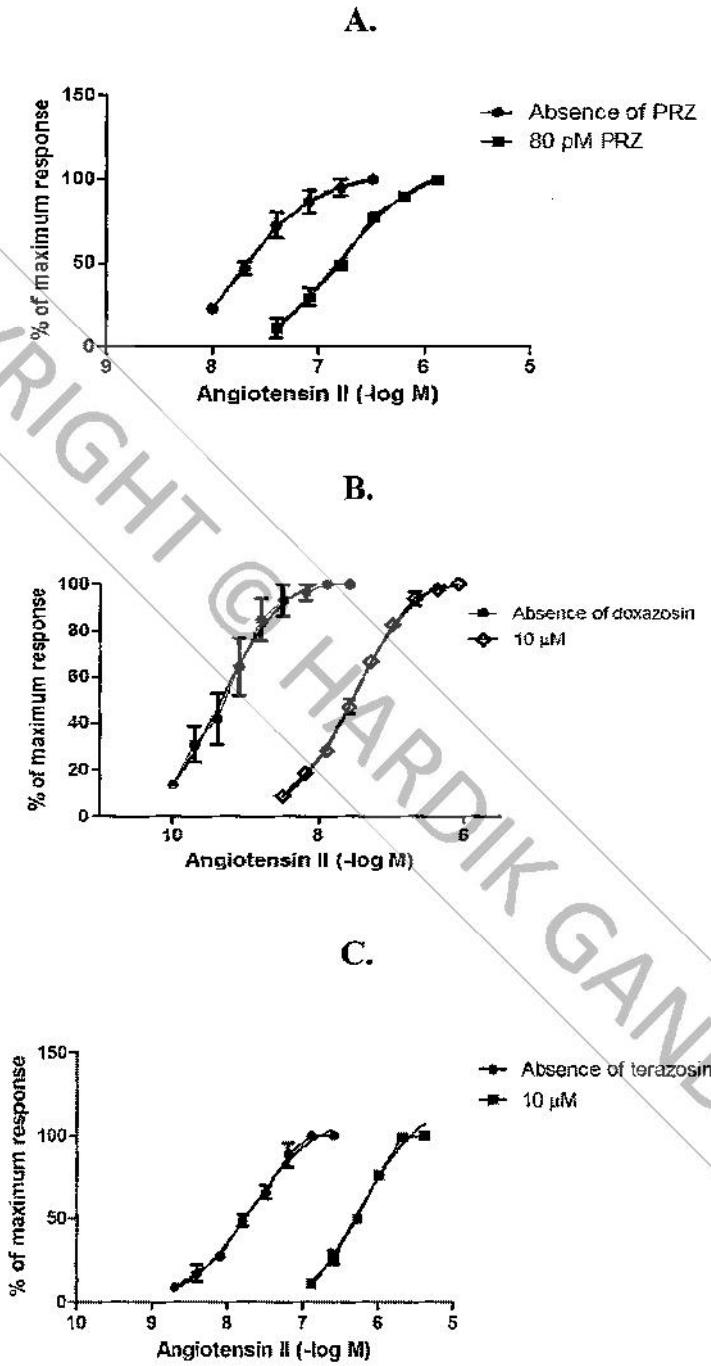




Figure 9: Concentration response curves of angiotensin II against, A) prazosin (80pM), B) doxazosin (10µM) and C) terazosin (10µM).

A.

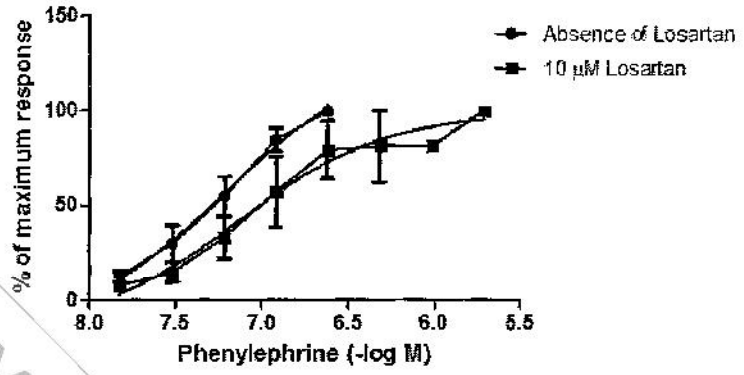


B.

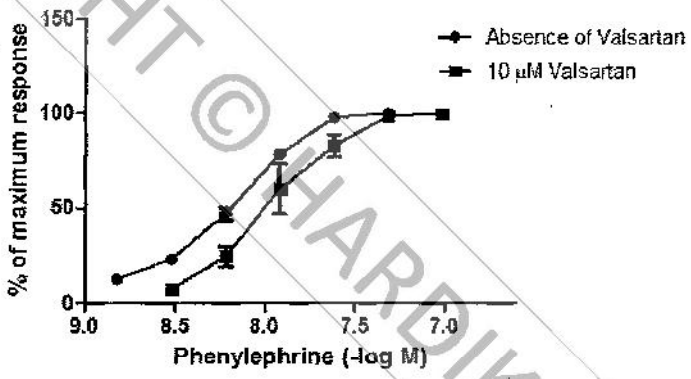


C.

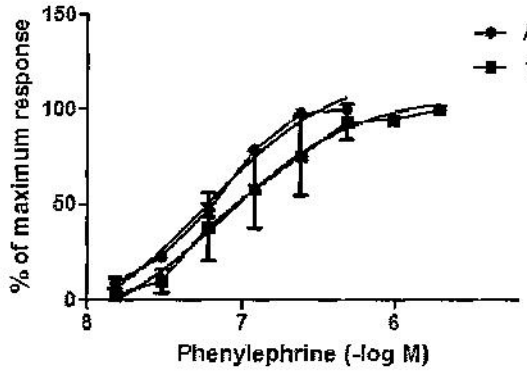


Figure 10: Concentration response curves of phenylephrine against, A) losartan (10µM), B) valsartan (10µM) and C) olmesartan (10µM).

***Screening of potential compounds for dual antagonism of $\alpha_1$- and angII- receptors antagonism***

Based on the studies with standard compounds and the encouraging results obtained therewith, it was decided to screen six series (I-VI) of compounds for potential dual antagonistic activity on the $\alpha_1$- and angII- receptors (Figure 11). Details about the series and the activity of different compounds therein are given in tables 5-10.

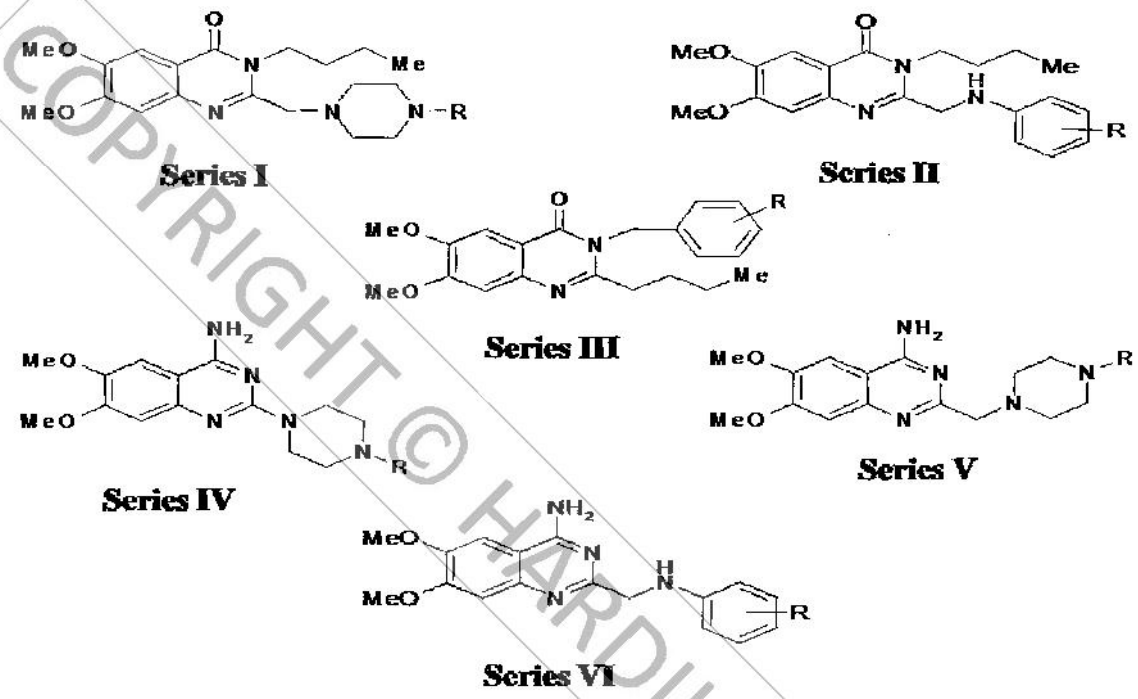


Figure 11: This figure represents the six series of compounds that were chosen as part of the preliminary screening protocol to identify a potential dual antagonist. 6, 7-Dimethoxyquinazoline ring system is native to all the series with series I-III being 4-keto derivatives and series IV-VI being 4-amino derivatives. Other differences are observed at the substitutions on 2nd and 3rd positions.

**Table 5: Preliminary studies on compounds of series I**

| Compound | 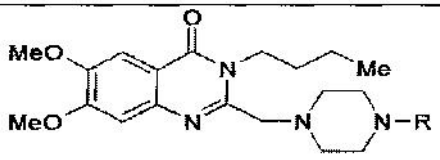 *Where –R is* | *p*$A_2$ values | |
|---|---|---|---|
| | | $\alpha_1$ | $AT_1$ |
| I-1 | $-CH_3$ | 4.18 ± 0.09 | NC |
| I-2 | $-CH_2CH_3$ | 5.28 ± 0.08 | NC |
| I-3 | $-C_6H_5$ | 5.45 ± 0.24 | 3.82 ± 0.09 |
| I-4 | $-C_6H_{11}$ | 6.22 ± 0.10 | 4.98 ± 0.09 |

| | | | |
|---|---|---|---|
| **I-5** | -$C_6H_4CN$ (*o*) | **7.71 ± 0.10** | **7.41 ± 0.10** |
| **I-6** | -$C_6H_4OCH_3$ (*o*) | 7.21 ± 0.09 | 5.03 ± 0.11 |
| **I-7** | -$C_6H_4F$ (*o*) | 6.33 ± 0.13 | 5.68 ± 0.05 |
| **I-8** | - $C_5H_4N$ | 6.49 ± 0.11 | 5.91 ± 0.15 |
| **I-9** | -$C_6H_4OH$ (*p*) | NC | 5.8 ± 0.09 |
| I-10 | -$CH(C_6H_5)_2$ | 6.07 ± 0.06 | NC |

**Table 6: Preliminary studies on compounds of series II**

| **Compound** |  *Where -R is* | **$pA_2$ values** | |
|---|---|---|---|
| | | **$\alpha_1$** | **$AT_1$** |
| **II-1** | -COOH (*m*) | 7.45 ± 0.16 | 6.14 ± 0.14 |
| **II-2** | -COOH (*p*) | 5.27 ± 0.28 | 5.75 ± 0.28 |
| **II-3** | -$NH_2$ (*p*) | 5.48 ± 0.15 | 5.28 ± 0.27 |
| **II-4** | -$NHSO_2CH_3$(*m*) | 6.06 ± 0.10 | 5.13 ± 0.33 |
| **II-5** | -$NHSO_2CH_3$(*p*) | 5.69 ± 0.29 | 5.62 ± 0.09 |
| **II-6** | -tetrazole *(m)* | 5.63 ± 0.21 | 4.9 ± 0.14 |
| **II-7** | -tetrazole *(p)* | 4.53 ± 0.08 | 5.19 ± 0.13 |

**Table 7: Preliminary studies on compounds of series III**

| **Compound** | 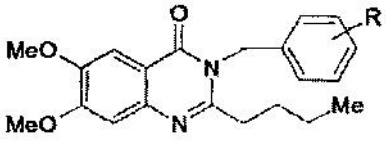 *Where -R is* | **$pA_2$ values** | |
|---|---|---|---|
| | | **$\alpha_1$** | **$AT_1$** |
| **III-1** | -$COOCH_3$ *(m)* | 6.42 ± 0.13 | 5.53 ± 0.11 |
| **III-2** | -$COOCH_3$ *(p)* | **6.97 ± 0.12** | **7.00 ± 0.11** |
| **III-3** | -COOH *(p)* | 5.50 ± 0.16 | 6.01 ± 0.21 |
| **III-4** | -$NO_2$ *(m)* | 7.13 ± 0.20 | 6.44 ± 0.15 |
| **III-5** | -CN *(m)* | 6.88 ± 0.13 | 6.65 ± 0.09 |
| **III-6** | -CN *(p)* | 6.40 ± 0.11 | 6.92 ± 0.12 |
| **III-7** | -tetrazole *(m)* | **7.10 ± 0.12** | **7.03 ± 0.12** |

**Table 8: Preliminary studies on compounds of series IV**

| Compound | 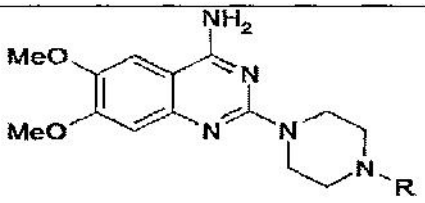 *Where –R is* | $pA_2$ values | |
|---|---|---|---|
| | | $\alpha_1$ | $AT_1$ |
| **IV-1** | -$CH_3$ | **9.23 ± 0.12** | 5.75 ± 0.07 |
| **IV-2** | -$CH_2CH_3$ | **10.41 ± 0.12** | 5.08 ± 0.08 |
| **IV-3** | -$C_6H_5$ | 8.74 ± 0.08 | 3.31 ± 0.13 |
| **IV-4** | -$C_6H_4CN$ (*o*) | **8.59 ± 0.51** | **9.04 ± 0.23** |
| **IV-5** | -$C_6H_4OCH_3$ (*o*) | 7.26 ± 0.12 | 6.54 ± 0.51 |
| **IV-6** | -$C_6H_4F$ (*o*) | 10.52 ± 0.14 | 5.52 ± 0.09 |
| **IV-7** | -$C_5H_4N$ | 6.95 ± 0.08 | 5.09 ± 0.12 |
| **IV-8** | -$CH(C_6H_5)_2$ | **7.09 ± 0.15** | **7.59 ± 0.58** |

**Table 9: Preliminary studies on compounds of series V**

| Compound | 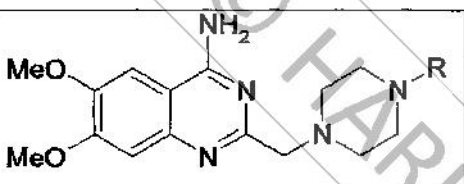 *Where –R is* | $pA_2$ values | |
|---|---|---|---|
| | | $\alpha_1$ | $AT_1$ |
| **V-1** | -$CH_3$ | 6.79 ± 0.22 | 5.1 ± 0.38 |
| **V-2** | -$CH_2CH_3$ | 4.19 ± 0.08 | 3.22 ± 0.10 |
| **V-3** | -$C_6H_5$ | 6.49 ± 0.13 | 6.78 ± 0.10 |
| **V-4** | -$C_6H_{11}$ | 4.90 ± 0.06 | 3.01 ± 0.25 |
| **V-5** | -$C_6H_4CN$ (*o*) | **10.1 ± 0.20** | **8.83 ± 0.38** |
| **V-6** | -$C_6H_4OCH_3$ (*o*) | **7.45 ± 0.09** | 6.34 ± 0.07 |
| **V-7** | -$C_6H_4F$ (*o*) | 6.76 ± 0.10 | 6.09 ± 0.13 |
| **V-8** | -$C_5H_4N$ | 5.47 ± 0.48 | 3.65 ± 0.15 |
| **V-9** | -$CH(C_6H_5)_2$ | 5.32 ± 0.07 | 6.36 ± 0.34 |
| **V-10** | -$C_6H_4COONa$ (*o*) | 3.64 ± 0.11 | 6.28 ± 0.28 |

**Table 10: Preliminary studies on compounds of series VI**

| Compound | 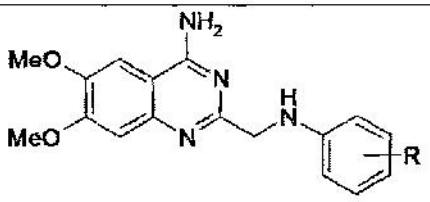 *Where –R is* | $pA_2$ values | |
|---|---|---|---|
| | | $\alpha_1$ | $AT_1$ |
| **VI-1** | -H | **9.87 ± 0.15** | **8.37 ± 0.43** |
| **VI-2** | -$CH_3$(*m*) | 6.16 ± 0.11 | 5.38 ± 0.14 |
| **VI-3** | -$CH_3$(*p*) | 5.28 ± 0.20 | 3.45 ± 0.34 |
| **VI-4** | -$OCH_3$(*p*) | NC | 6.29 ± 0.10 |
| **VI-5** | -COOH(*m*) | 5.52 ± 0.36 | 4.87 ± 0.17 |
| **VI-6** | -COOH(*p*) | 4.49 ± 0.20 | 6.43 ± 0.38 |
| **VI-7** | -$COOCH_3$(*m*) | 6.37 ± 0.13 | 6.27 ± 0.10 |
| **VI-8** | -$COOCH_3$(*p*) | 6.86 ± 0.12 | **10.64 ± 0.10** |
| **VI-9** | -$NO_2$(*m*) | **9.38 ± 0.18** | **7.64 ± 0.46** |
| **VI-10** | -$NO_2$(*p*) | **8.09 ± 0.12** | **9.04 ± 0.15** |
| **VI-11** | -$NHSO_2CH_3$(*m*) | 4.48 ± 0.29 | 3.41 ± 0.21 |
| **VI-12** | -$NHSO_2CH_3$(*p*) | NC | 4.38 ± 0.44 |
| **VI-14** | -$NHCOCH_3$(*p*) | 6.67 ± 0.12 | NC |
| **VI-15** | -Cl(*m*) | 7.02 ± 0.08 | 6.27 ± 0.12 |
| **VI-16** | -Cl(*p*) | 4.89 ± 0.27 | 4.65 ± 0.28 |
| **VI-17** | -Br(*m*) | 6.78 ± 0.14 | 7.23 ± 0.12 |
| **VI-18** | -Br(*p*) | 6.33 ± 0.10 | 6.75 ± 0.23 |
| **VI-19** | -F(*p*) | 6.60 ± 0.11 | 7.70 ± 0.20 |
| **VI-20** | -Naphthyl | **8.37 ± 0.27** | **7.07 ± 0.16** |
| **VI-21** | -$C_5H_4N$(*o*) | 6.91 ± 0.23 | 5.90 ± 0.14 |
| **VI-23** | -$C_5H_4N$(*p*) | 5.86 ± 0.13 | 4.68 ± 0.09 |
| **VI-24** | -morpholinyl | 5.26 ± 0.16 | 6.15 ± 0.25 |
| **VI-25** | -$C_5H_{10}N$ | 3.01 ± 0.06 | 3.70 ± 0.17 |
| **VI-26** | -triazolyl | 5.93 ± 0.13 | 5.47 ± 0.13 |
| **VI-27** | -$C_4H_8N$ | 3.49 ± 0.07 | 3.63 ± 0.08 |
| **VI-28** | -$C_7H_5N_2$ | 4.05 ± 0.10 | 4.15 ± 0.12 |

Based on the results of these preliminary findings, a few compounds were shortlisted as potential antagonists exhibiting dual antagonism of α1-adrenoceptors and angII receptors. These compounds included I-5, III-2, III-7, IV-4, IV-8, V-5, V-6, VI-1, VI-9, VI-10 and VI-20 (marked **bold** in the tables). Out of these compounds, V-5 was selected for further studies as it was found to demonstrate most potent antagonism at both the receptors in question and the activity was even better than prazosin and losartan on the $\alpha_1$-adrenoceptors and angII receptors respectively. This compound was further coded as ***MCR-1329*** as per coding norms of our laboratory.

***Elaborated functional antagonism assay of potent compound***

The antagonism afforded by **MCR-1329** on rat aortic strips was evaluated at 3 different concentrations (1, 5, 10 μM) only to find that each higher concentration resulted in a further rightward parallel shift in the CRC of phenylephrine as well as angII. It has been suggested that if a series of antagonist concentrations yield linear Schild regression with a slope of unity, then the $pA_2$ vlaue obtained may be considered as the actual affinity of the ligand to the receptor (Kenakin, 2009; Dale and Haylett, 2009), otherwise at a single concentration, *p*A2 value remains only an empirical measure of antagonist potency (Kenakin, 2009). The $pA_2$ value calculated at different concentrations of **MCR-1329** remained the same as that observed in preliminary studies. Accordingly, the $pA_2$ value of **MCR-1329** against phenylephrine mediated contractions was 10.10 ± 0.20 (Figure 12A) and for that against angII was found to be 8.83 ± 0.38 (Figure 12B).

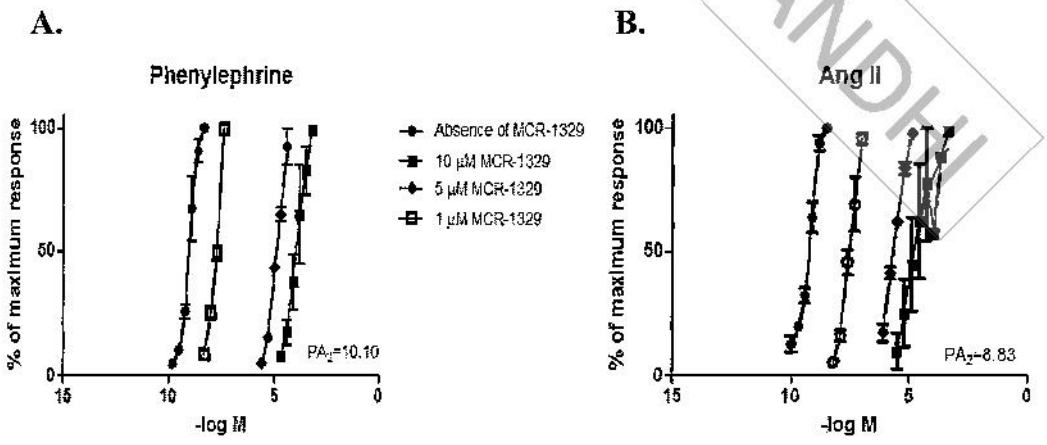


Figure 12: Concentration response curves to phenylephrinne (A) and angiotensin II (B) in presence of different concentrations of **MCR-1329** (0, 1, 5, 10 μM).

## *IN VIVO* PRESSOR RESPONSE EVALUATION

### *Unmasked pressor response*

The effects of **MCR-1329** *in vitro* were so profound that it was decided to challenge it against the *in vivo* effects of phenylephrine and angII on rat arterial blood pressure. Intact animals have been utilized by different research groups to evaluate the effects of angII (Liles *et al*, 2006; Padia *et al*, 2006) and phenylephrine (Smith *et al*, 2006; Cunha *et al*, 2005) on arterial blood pressure. This method involves measurement of arterial blood pressure after cannulation of the carotid artery and offers a direct measurement of blood pressure (Kurtz *et al*, 2005). This method may also be used to study arterial reactivity. Accordingly, two dose levels were chosen and the effects of **MCR-1329** were evaluated against intravenous injections of phenylephrine and angII (6µg/kg, i.v. each). The effects were compared with equimolar doses of prazosin and losartan as standards. It was found that prazosin-mediated effects were stronger as compared to **MCR-1329** in inhibiting the pressor response to phenylephrine. At a lower dose of 0.36 µmol/kg, prazosin exhibited near 50% inhibition of pressor response to phenylephrine whereas **MCR-1329** showed about 20% inhibition. At higher doses (0.72 µmol/kg), the effects were more prominent and prazosin almost completely blocked the pressor effects of phenylephrine while **MCR-1329** also significantly blocked the responses of phenylephrine to about 70% (Figure 13A). Separate dose levels were employed for the evaluation of antagonistic effects of losartan and **MCR-1329** against angII mediated pressor responses. Evaluation of mean arterial pressures revealed that losartan at a dose level of 0.72 µmol/kg produced around 50% inhibition of the pressor response to angII. At an equimolar dose the response of **MCR-1329** may be considered feeble and produces only about 10% inhibition of pressor response. Administration of 3.6 µmol/kg losartan prior to angII challenge brought about a complete inhibition of angII mediated rise in blood pressure. However, **MCR-1329** negotiated only about 40% inhibition of pressor response at the equimolar dose (Figure 13B). The results were intriguing since there was a vast difference between the *in vitro* data and preliminary *in vivo* investigations.

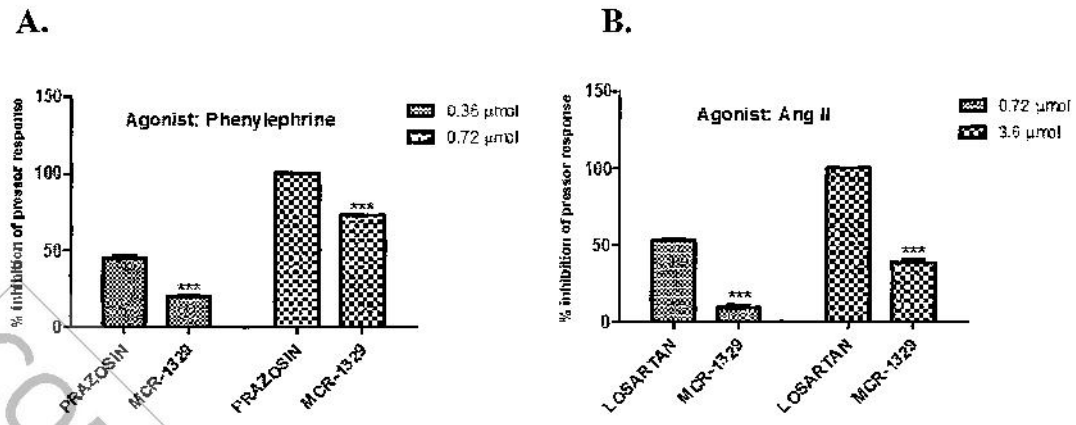


Figure 13: Mean arterial pressor response inhibition of phenylephrine (A) and angiotensin II (B) in animals previously dosed with **MCR-1329** or standards at equimolar levels (prazosin for phenylephrine and losartan for angiotensin II).

While *in vitro* data showed quite high potency of the test compound, **MCR-1329**, which was even higher than the standard compounds, results from the *in vivo* studies did not concur the same. This uncertainty was deliberated upon and the causes for such inconsistency were evaluated. It was presumed that probably **MCR-1329** undergoes rapid metabolism in the blood stream leading to a laid-back inhibition of pressor response. This was unlikely since the standard and test drugs were injected intravenously and the effects were observed immediately upon administration. Thus it could be a rare possibility that **MCR-1329**, a quinazoline derivative is metabolised immediately in contact with blood. Another speculation was that **MCR-1329** undergoes extensive plasma-protein binding, which prevents the compound from binding to the respective receptors. This was more likely to happen as it is known that derivatives of quinazoline are known to undergo extensive plasma protein binding. An *in vitro* study was planned to compare the plasma protein binding profiles of prazosin, losartan and **MCR-1329**. The results of this study revealed that this compound does not have major difference between itself and prazosin w.r.t plasma protein binding. The results of this study are presented in detail in the *PHARMACOKINETICS* section. On the basis of protein binding studies, lesser *in vivo* potency of **MCR-1329** could not be explained.

While mulling over these alternatives, one fact was clearly overlooked. Since **MCR-1329** shows dual action *in vitro*, it is possible that the actual concentration of the drug reaching at a particular receptor was much lesser while administering the drug on a molar basis. The reasons for such an abridged response may therefore be the

distribution of the drug upon both the receptors in question suggesting that only a fraction of **MCR-1329** is available at a given time to act upon a particular population of receptors since **MCR-1329** was designed as a multitargeted ligand. Multitargeted ligands are particularly suggested for conditions that have manifold etiopathologies so that a single agent can be utilized for direct inhibition of the causative factors. This fact may be correlated with several other investigational multitargeted ligands studied for the likely management of complex diseases (Wei *et al*, 2008; Bajda *et al*, 2011) which show differential inhibition of the targets involved (Bolognesi *et al*, 2010).

This speculation was based on *in vitro* studies performed earlier on isolated rat aortic strips. In those experiments, **MCR-1329** showed competitive antagonism against phenylephrine and angiotensin II, respective specific agonists of the $\alpha_1$- and AII-receptors. This was evident from the rightward parallel shift observed in the dose-response plots for **MCR-1329**. This competitive inhibition of the contractile response in isolated vascular tissue showed that **MCR-1329** had the ability to bind to both the receptors in question in a dose-dependent manner. This condition of competitive binding to both the receptors was expected to be prevalent in the *in vivo* model as well, thereby causing reduction in the inhibition response of **MCR-1329** on both the receptors in comparison to the standard drugs. However, with this speculation it was not assumed that **MCR-1329** might show an equivalent distribution on both the receptors in question and hence the disparity among responses to phenylephrine and angII remained open to experimental conclusion. The reflection of this hypothesis is directly seen from the results which show that equimolar doses of **MCR-1329** show lesser amount of inhibition when compared to prazosin or losartan.

***Masked pressor response***

To provide credence to the hypothesis proposed above, it was planned to evaluate the pressor-inhibition potential of **MCR-1329** under masked conditions. *In vivo* inhibition of phenylephrine mediated arterial pressor response by **MCR-1329** was measured in those animals in which 12.5 mM losartan was pre-administered. The idea behind such a protocol was to mask the effects of **MCR-1329** on angII receptor. Similarly, the other set involved measurement of inhibition of angII mediated arterial pressor response in those animals in which 400 µM prazosin was pre-administered to mask the effects of **MCR-1329** upon $\alpha_1$ receptor. The drugs and standard compounds

were administered at equimolar concentrations. Such a protocol for studying the effects of agonists under masked conditions has not been reported in the literature previously. The results obtained are shown in figure 14.

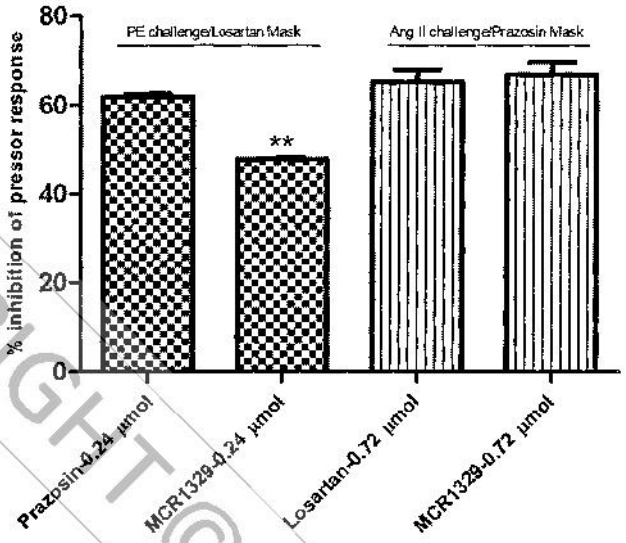


Figure 14: Mean arterial pressor responses to phenylephrine under losartan masking (checkerd columns) and to angII under prazosin masking (ruled columns). In case of phenylephrine challenge, the effect of **MCR-1329** was found to be moderate in comparison to prazosin.

It can be observed that the hypothesis stands true as **MCR-1329** was equipotent to losartan after masking the $\alpha_1$-receptors with prazosin and slightly less active than prazosin after masking A-II receptors with losartan. Though compartmentalization of the drug was excluded with the possibility of high-degree of plasma protein binding (Roberts *et al*, 2013), the disparity of receptor distribution could not be ruled out. Disparities in receptor distribution owing to different receptor densities have been studied previously on neuropeptide (Beaudet *et al*, 1998) and cannabinoid receptors (McPartland *et al*, 2007).

As stated above, we have previously shown that prazosin shows potent antagonism of the angII receptors as well. Such type of action is responsible for an enhanced antihypertensive response afforded by prazosin. However, this effect can play a dual role in our masking study, again by acting on both $\alpha_1$ and angII receptors. Hence we performed the same study using terazosin as a standard $\alpha_1$ antagonist (Figure 15), which we have shown to have negligible action on angII mediated

vascular smooth muscle contraction. Activity of terazosin is exclusive for the $\alpha_1$ receptor and hence we can safely assume that the effects of terazosin are mediated due to binding with $\alpha_1$ receptor only. No significant differences could be observed between the effects of terazosin (as a masking agent and a standard $\alpha_1$-antagonist) and that of **MCR-1329** as shown in figure 15.

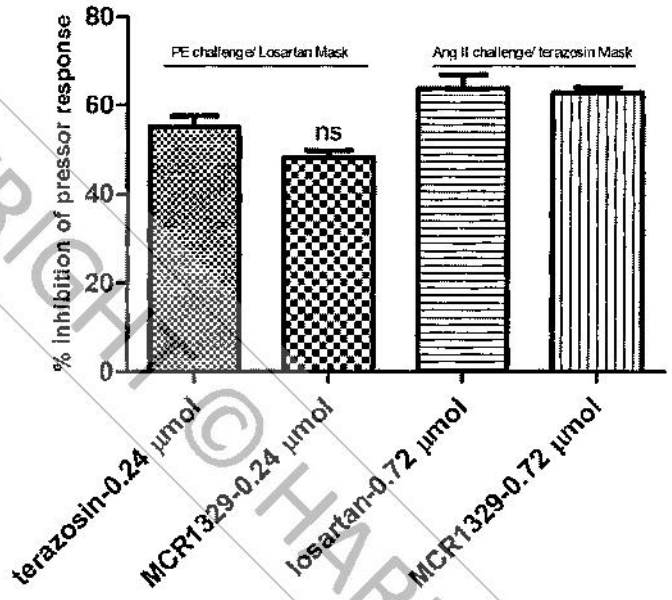


Figure 15: Mean arterial pressor responses to phenylephrine under losartan masking (checkered colums) and to angII under terazosin masking (ruled columns). In case of phenylephrine challenge, the effect of **MCR-1329** was found to be statistically comparable without any significant difference.

Such a masking study has not been reported in the literature. The results clearly shed light on the multiple effects shown by drugs used in clinical practice. The results suggest that the drugs used in clinical practice may have certain off-target effects not known at present. Simultaneously, it is also evident that it is possible to design ligands which have multiple targets for action. Such compounds may form the basis for favourable management of complex disorders like hypertension, atherosclerosis, alzheimer's and the like.

## TOXICOLOGICAL EVALUATION OF MCR-1329

***Single dose acute oral toxicity***

Studies with different quinazoline derivatives have not shown any untoward toxicity signs belonging to this class of compounds (Zayed and Hassan, 2013; Alafeefy *et al*, 2010; Sinha *et al*, 2013). These studies have reported a safety of assorted quinazoline derivatives upto 2000 mg/kg and beyond. However, to ensure the safety of the test compound, **MCR-1329** was administered at the recommended dose. The post-treatment examination period was 14 days from the date of dosing. Body weights of the animals were recorded on days 0, 7 and 14. Slight fluctuations were observed in the body weight of animals but since they were within 20% of the mean body weight no additional measurements were taken and any other precaution was not followed. The animals were closely observed during the first 6 hours after dosing. The animals were starved during this period with access to water. No significant observations were recorded during this period. This part coincided with the light cycle and most of the time animals were asleep. When awake, the animals showed normal grooming behavior and water intake was also normal. During the entire post-treatment observation period special attention was paid to alteration of skin or fur, abnormal locomotion or breathing and changes in the eye. No untoward observations were made in this regard until the terminal day of the study. Mortality was recorded twice daily but no mortality was found in any dose group till day 14. At the end of the study period, the animals were euthanized and major organs (brain, heart, lung, liver, kidney, spleen) were harvested. Gross necropsy was performed by an individual blinded to the groups. No macroscopic lesions were recorded. Viscera, gastrointestinal tract and mucous linings appeared normal. Major blood vessels did not show any abnormalities. Detailed report on toxicity evaluation is presented as Appendix I.

Administration of 2000 mg/kg of **MCR-1329** showed no signs of toxicity or mortality during the test period. The $LD_{50}$ of **MCR-1329** in rats was thus found to be >2000mg/kg.

***Repeat dose oral toxicity***

At the end of the study, no untoward observations were made regarding body weight, food intake or normal behavior. Gross necropsy did not reveal any suggestive lesions or abnormal anatomical feature. The most plausible side effect related to the mechanism of action of **MCR-1329** is hypotension. This effect was not evident from the tail-cuff recordings. Biochemical estimations did not suggest any major digression

from normal values. Urinary output and hematological data appeared normal. Studies with other quinazoline derivatives like fenazaquin have shown that this class of compounds is safe for daily administration upto a dose level of 30 mg/kg/day (Francis *et al*, 1992). Detailed report on repeat dose toxicity evaluation is presented as Appendix II. It was concluded that chronic administration of **MCR-1329** at a dose level of 10 mg/kg was safe.

## PHARMACOKINETIC STUDIES

### *HPLC method*

The HPLC analysis of prazosin and related quinazoline compounds has been successfully attempted by different researchers. Sultana *et al* (2013) has reported the analysis of prazosin by HPLC as API, in dosage forms and serum samples using a mobile phase composition of acetonitrile : water (75:25, *p*H=3.2). Ahmed *et al* (2010) showed the extraction and estimation of prazosin hydrochloride from pharmaceutical dosage forms using a mobile phase composition of 20 mM OPA: acetonitrile (70:30, *p*H=2.5). In both the analyses, the wavelength of detection was 254 nm. Shrivastava and Gupta (2012) have reported a method for simultaneous estimation of prazosin, doxazosin and terazosin. Rao *et al* (2006) also developed a method which could be applied to the quality assurance of 6,7-dimethoxyquinazolines. Before establishing the HPLC method for our test compound, several trials were performed to optimize the parameters for analysis of **MCR-1329** on HPLC. 10 mg of **MCR-1329** was dissolved in 10 ml of 0.1% OPA by vortexing to give a final concentration of 1 mg/ml. 0.1% of OPA was used as a blank solvent. Spectral scan of the stock solution on UV-1800 (Shimadzu, Japan; scan range 200-400 nm) gave the following data (Table 11):

**Table 11: Absorbance of MCR-1329 at different wavelengths**

| Wavelength (nm) | OD |
|---|---|
| 220 | 1.019 |
| ***243*** | ***0.833*** |
| 254 | 0.754 |
| 323 | 0.352 |

Different wavelengths have been utilized in the literature for estimation of quinazoline derivatives by HPLC. While Sultana *et al* (2013) utilized 254 nm for prazosin, Rao *et al* (2006) studied dimethoxyquinazolines at 240 nm. The Indian Pharmacopoeia and its European counterpart both indicate that 254 nm be used as the wavelength for estimation of prazosin. Based on these values and our observations 243 nm was selected as the wavelength for estimation since it showed the highest absorbance after 220 nm in the spectral scans. 220 nm was not chosen as the λmax for estimation since this wavelength falls below the UV cut-off of several organic solvents which are commonly used as mobile phases for HPLC.

Next, several mobile phases were tried based on the data available for related class of compounds. Different mobile phase compositions evaluated to obtain a good resolution for **MCR-1329** are shown in table 12.

**Table 12: Mobile phase combinations evaluated for elution of MCR-1329**

| Mobile Phase ID | Solvent Mixture | Ratio |
|---|---|---|
| I | Methanol: Water (*p*H=6) | 50:50 |
| II | Acetonitrile: Methanol: Water (*p*H=6) | 10:70:20 |
| III | Acetonitrile: Methanol: Water (*p*H=6) | 10:55:35 |
| IV | Acetonitrile: Methanol: Water (*p*H=6) | 22:22:56 |
| V | Acetonitrile: Methanol: Water (*p*H=6) | 20:40:40 |
| VI | Acetonitrile: 0.2% OPA (pH=3) | 40:60 |
| ***VII*** | ***Acetonitrile: 0.04M $Na_2HPO_4$ (pH=3)*** | ***40:60*** |
| VIII | Acetonitrile: Methanol: 0.04M $Na_2HPO_4$ (*p*H=3) | 20:70:10 |

Mobile phase I through V were chosen based on the solubility of **MCR-1329** in these mobile phases without the need for adjusting an acidic *p*H. Mobile phase II showed better solubility at normal *p*H of distilled water. However, when **MCR-1329**

was eluted using these mobile phases, very broad peaks were obtained. With mobile phases III & IV, tailing was also observed. It is known that *p*H of the mobile phase and its composition can be useful parameters in determining the elution of an analyte based on its *p*Ka value (Heinisch and Rocca, 2004). It was thus decided to use an acidic mobile phase for better and faster resolution of the test compound. **MCR-1329** was easily eluted in mobile phases VI-VIII, the reason being enhanced solubility due to an acidic *p*H. In some cases, it was found that lower concentrations of the test compound (below 10 ppm) were not resolved properly. The peak intensity and $R_t$ of the analyte fluctuated on a case-to-case basis, i.e change in mobile phase and flow rate adjustments. No such problems were observed with mobile phases VII and VIII. Analyte peaks obtained with mobile phases VII and VIII were sharp, symmetric and free from tailing or shouldering effects. It was finally decided to utilize mobile phase VII for the purpose of analysis simply because of the relative ease of preparation.

Flow rate is known to affect not the resolution but only the retention time of the analyte in HPLC (Pous-Torres *et al*, 2009). Flow rate adjustments showed that a flow rate of 0.8 ml/min gave a peak between Rt of 3.5-4.5 mins, so that the time of actual analysis would be less than 5 mins, however, for the sake of brevity the time of analysis was kept 15 min. Most of the times, the analyte was eluted at an $R_t$ of 4.2 ± 0.1 min. An $R_t$ of less than 3 min at this flow rate would mean that the analyte is eluted in the dead volume of the 250 mm column. This combination of mobile phase and flow rate gave a

**Table 13: Optimized HPLC parameters for quantification of MCR-1329**

| | |
|---|---|
| System | Shimadzu make |
| Column | Octadecyl silane (C18), Purospher |
| Mobile phase | ACN: 0.04M $Na_2HPO_4$ (*p*H=3); 40:60 |
| Flow rate | 0.8 ml/min |
| Pressure | 108 ± 6 kgf |
| Injection Volume | 20 µl |
| Temperature of analysis | 25 ± 2°C |
| Detection wavelength | 243 nm |
| Retention time ($R_t$) | 4.2 ± 0.1 mins |
| Run time | 15 mins |

pressure of about 108 ± 6 *kgf* on the column which was of sufficient length for the analysis. Extraction efficiency of the sample preparation method was found to be greater than 90% at evaluated concentrations. The optimized HPLC conditions are summarized in the table 13.

***Construction of calibration curves and linearity***

Based on these parameters, calibration curves were constructed for **MCR-1329**. Two calibration curves were constructed, first after dissolving known amount of **MCR-1329** in mobile phase and preparing aliquots by serial dilutions (62.5-1000 ng/ml) and the second by spiking rat plasma samples from control animals with known amounts of **MCR-1329** (62.5-1000 ng/ml) and following the entire sample extraction and preparation procedure. The chromatograms, graphs, regression equations and linear correlation coefficient values for the same are presented in figures 16-19 below:

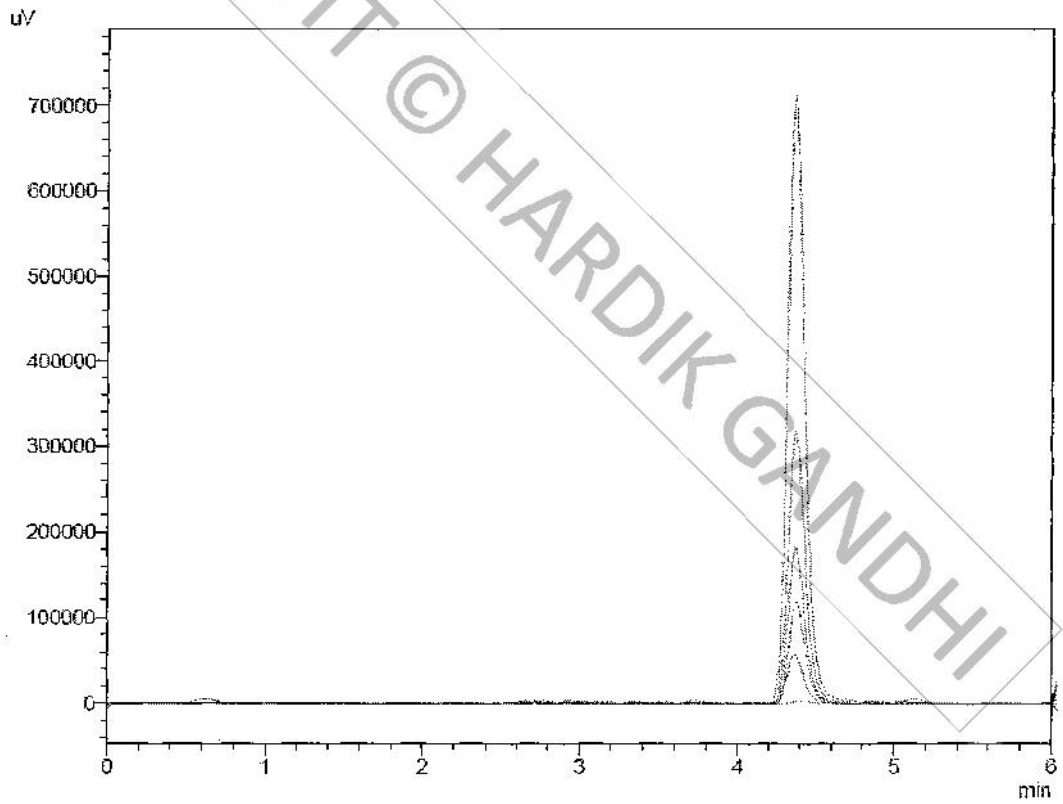


Figure 16: Chromatogram showing an overlay of peaks for calibration curve of analytical aliquots of the **MCR-1329**. The abscissa represents time in mins while the ordinate represents peak intensity in microvolts.

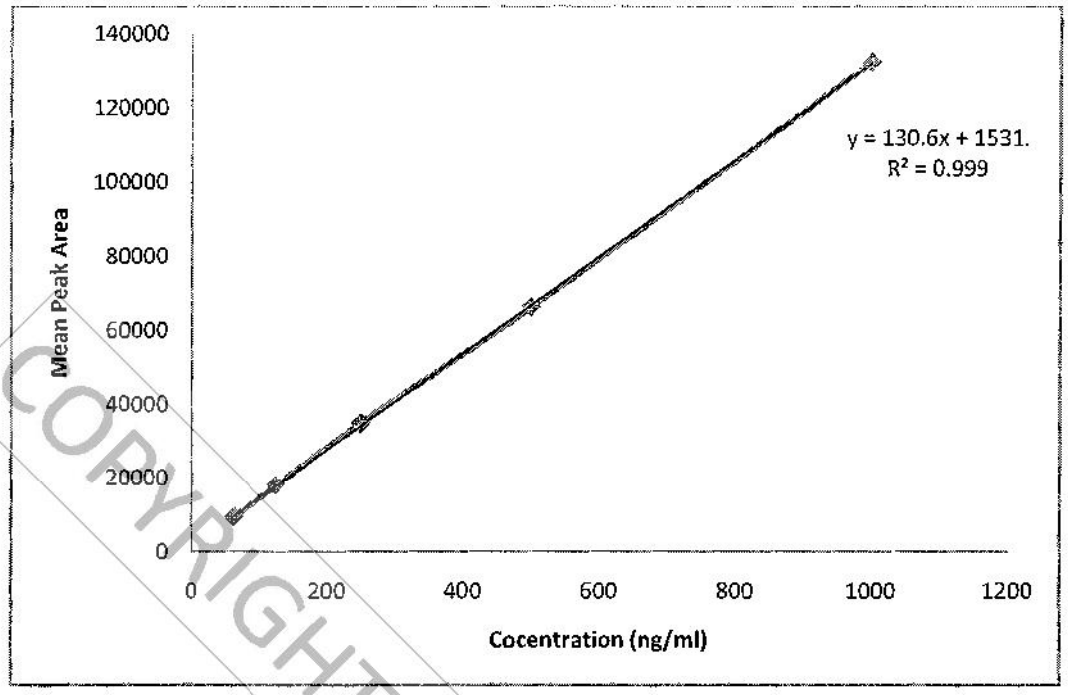


Figure 17: Calibration curve of **MCR-1329** from analytical samples dissolved in mobile phase. This graph was plotted using mean peak areas obtained for each peak at different concentrations.

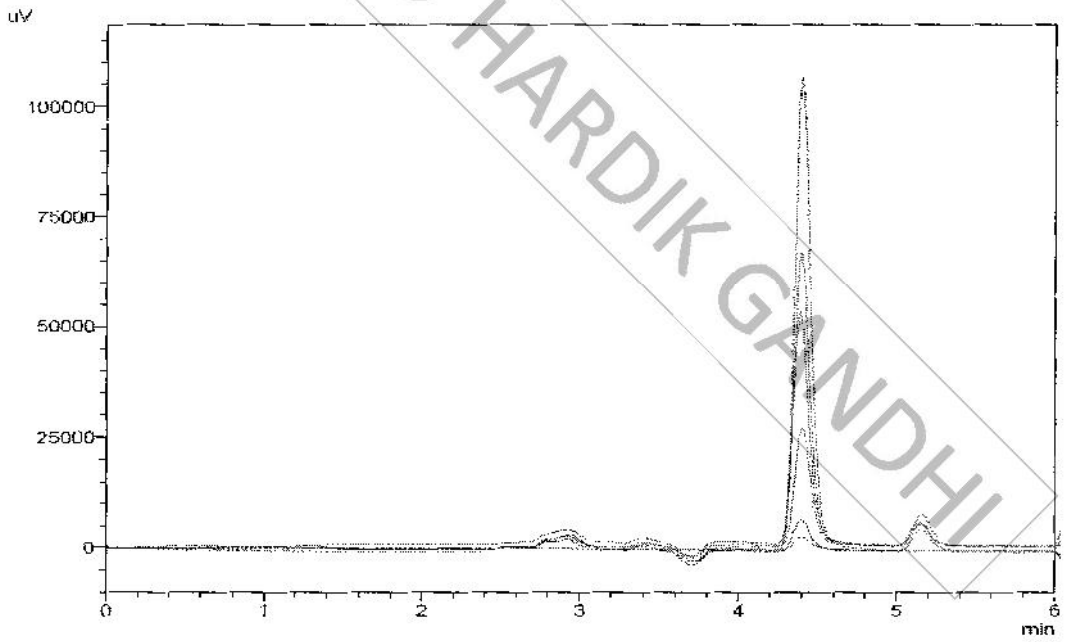


Figure 18: Chromatogram showing an overlay of peaks for calibration curve of spiked plasma samples. The abscissa represents time in mins while the ordinate represents peak intensity in microvolts.

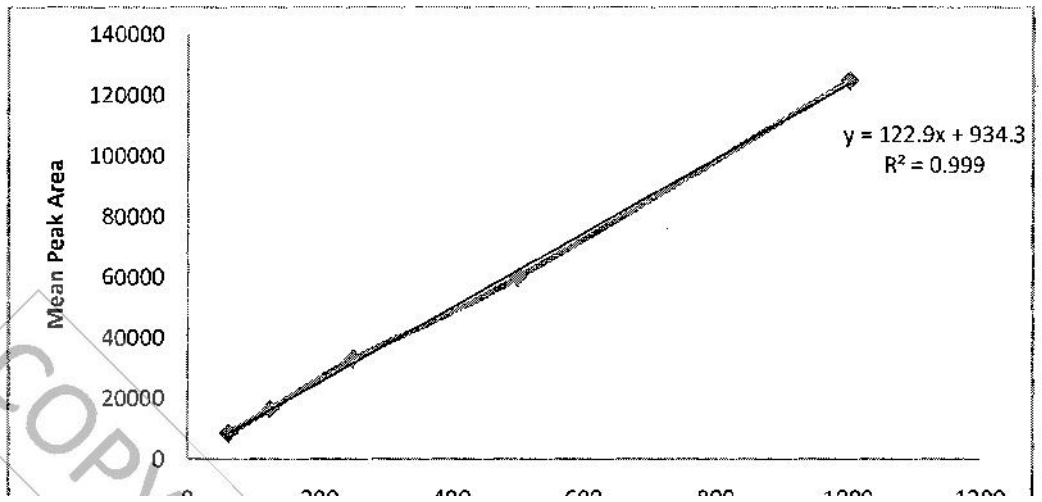
140000
120000
100000
80000
60000
40000
20000
0
Mean Peak Area
y = 122.9x + 934.3
R² = 0.999

CDER guideline for bioanalytical methods (USFDA) indicating that the method is accurate and can be used for the quantification of **MCR-1329**. All RSD values for intra-day and inter-day precision fell within 5% which is again in agreement for the bioanalytical methods (Table 14). No major fluctuation was observed in the signal, and analyses between days were in close conformity with each other.

***Oral dose disposition analysis***

The mean concentration time course of **MCR-1329** after oral administration is shown in figure 20. The curve shows an asymmetric morphology, a deviation from the Gaussian distribution, suggesting that the elimination phase is prolonged and lasts longer as compared to the absorption phase. The fluctuations obtained at different concentrations may be a result of the dose adjustments made as per the body weight of animals used in replicate analysis. There is absence of any trough and a single peak is obtained, which indicates that the test compound is highly bound to plasma proteins and does not leave the vascular compartment. Binding of **MCR-1329** to plasma proteins was observed in a separate *in vitro* study. A shouldering concentration is found at 10 hrs after oral administration, which seems incidental since the remaining curve does not present any anomalies w.r.t disposition of **MCR-1329**. Measurable levels of **MCR-1329** were present in the serum upto 24 hr post dose but not beyond 28 hr. Overall, the results suggest that **MCR-1329** is rapidly absorbed from the stomach and upper part of the intestine after oral administration and is eliminated at a rate which is moderate as

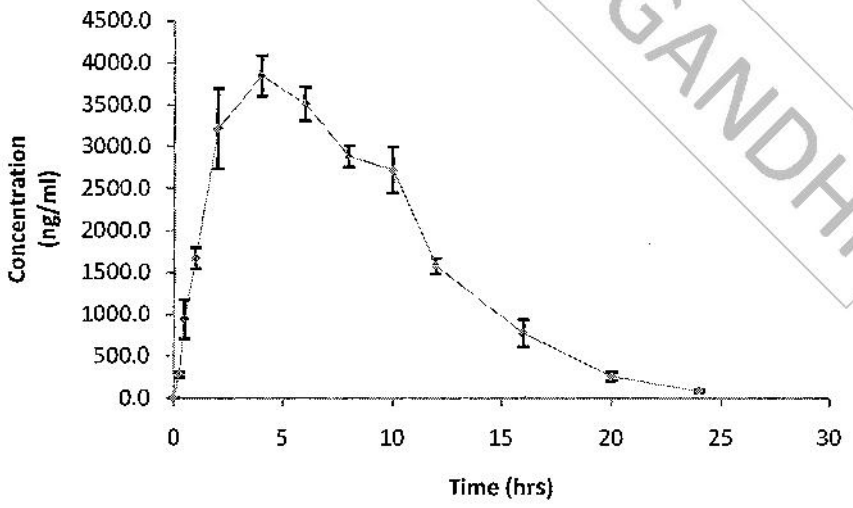


Figure 20: The figure shows the plasma concentration v/s time profile of **MCR-1329** after oral administration to rats (10 mg/kg, n=6).

compared to the absorption rate. The results obtained herewith can be interrelated with associated compounds like prazosin and other dimethoxyquinazolines (Chen *et al*, 1999; Sripalakit *et al*, 2005; Jaillon, 1980). Model independent pharmacokinetic parameters are listed in table 15.

**Table 15: Summary of pharmacokinetic data based on non-compartmental model**

| Parameter | Dose (10 mg/kg) |
|---|---|
| $C_{max}$ (ng/ml) | 3840.8 ± 241.4 |
| $T_{max}$ (hr) | ~ 4.0 |
| $K_{el}$ ($h^{-1}$) | 0.184 |
| $t_{1/2}$ (hr) | 3.77 |
| MRT (hr) | 7.68 |
| $AUC_{0-24}$ (ng.h/ml) | 41495.9 |
| $AUC_{0-\infty}$ (ng.h/ml) | 41505.1 |

***Human plasma protein binding study***

**MCR-1329** was allowed to bind to human plasma proteins present in pooled plasma and later on the release of this bound **MCR-1329** across a semi-permeable membrane was studied over a period of time. It was found that **MCR-1329** was gradually released into the stirred layer through the semi-permeable membrane as the bound form remained in equilibrium with the stirred layer which did not contain any amount of **MCR-1329**. The figure indicates the time-course of release of **MCR-1329** over a period of 24 hrs. It may be observed that even after 24 hrs of stirring (with sink conditions maintained by replacing fresh buffer), nearly 40% of **MCR-1329** still remained bound to the proteins in the plasma and was not released in the stirred layer (Figure 21). This study suggested that **MCR-1329** might remain in the vascular compartment upon absorption since it is highly bound to plasma proteins. As per the findings of the present study with **MCR-1329**, other dimethoxyquinazolines have been found to show a high degree (>90%) of plasma protein binding. Hence the results in this regards are in agreement with findings of other quinazoline derivatives (Jaillon, 1980; Uckun *et al*, 1999).

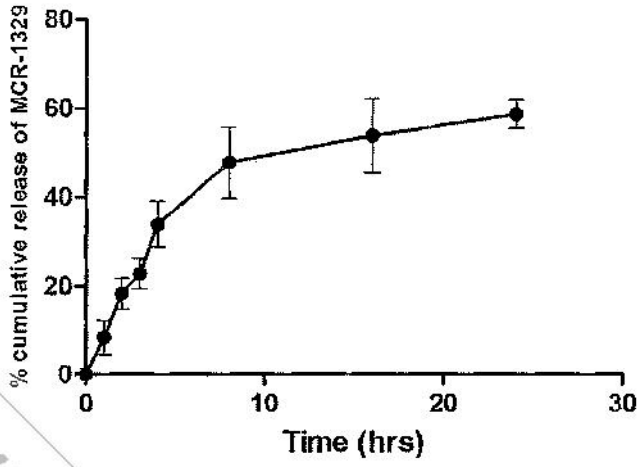


Figure 21: Time course of release of **MCR-1329** from human plasma protein binding. It is important to note that even after 24 hrs more than 40% **MCR-1329** remained bound to the plasma proteins and the slope of the curve is reduced after about 8 hrs.



## DOCA SALT MODEL

### *MCR-1329 abates rise in blood pressure*

*Tail-cuff data*

Pre-induction tail-cuff recordings showed that nearly all the animals utilized for the study were normotensive and no extreme levels of systolic blood pressure were recorded. DOCA administration alongwith salt intake is known to induce renal hypertension related to its sodium water retention effects (Seifi *et al*, 2010). DOCA being the precursor to aldosterone, is converted to aldsoterone *in vivo* through the action of the enzymes 11β-hydroxylase and subsequently aldosterone synthase. This *de novo* formation of aldosterone from exogenously aldministered DOCA leads to sodium retention in the distal tubules of the kidney (Iyer *et al*, 2010; Tomaschitz *et al*, 2010). However, the effects of such an exogenous administration may not be perceived until DOCA administration is also accompanied by salt intake (Badyal *et al*, 2003). Increase in blood pressure is mediated mainly through plasma volume expansion accompanied by sympathoexcitation and increased vasopressin levels (O'Donaughy and Brooks, 2006). Alteration of the central baroreflex (Schenk and McNeill, 1992), involvement of NOX pathways (Iwashima *et al*, 2008) and endothelin-I induced vasoconstriction (Callera *et al*, 2003) are also signatory to DOCA-salt mediated hypertension.

Severe hypertension was induced in the animals treated with DOCA-Salt (>160 mm Hg, $P<0.001$) towards the end of the study, whereas the UNX group showed non-significant rise in blood pressure (97.33 ± 2.22 v/s 108.3 ± 3.63 mm Hg). Control animals remained normotensive throughout the duration of the study. Animals treated with **MCR-1329** showed that **MCR-1329** was able to nullify the effects of DOCA-salt mediated renal hypertension and a 4-week regimen could conclude the antihypertensive effects of **MCR-1329** in animals. Likewise, the standard group also showed the beneficial effects of prazosin and losartan combination in animals treated with DOCA-salt. Figure 22 shows that there is scarcely any difference between the blood pressure values of the standard and the test group.

*Invasive recording data*

Intraarterial recordings were also comparable to those of the tail-cuff ones. Mean arterial pressure recordings showed that there was a difference of more than 60 mmHg units between the control and DOCA-salt group. Since pre-induction and post-induction levels could not be compared the terminal MAPs were directly evaluated by one-way ANOVA. The results indicated that DOCA-salt treated animals had significantly higher MAPs as compared to control and UNX animals whereas the treated animals (**MCR-1329** or standard combination) showed significant prevention in the elevation of MAP (Figure 23). Several studies have shown that unilateral nephrectomy induces negligible rise in blood pressure as compared to control animals (Giachini *et al*, 2011; Ndisang and Jadhav, 2010) which are in agreement with the results of the present study. No difference was observed between the pressure levels of **MCR-1329** and the standard group. As a matter of fact, the MAPs from the treatment groups were in close agreement with the UNX group suggesting that the treatments invalidated the hypertensive effects of DOCA salt. Since the molecular weights of **MCR-1329**, losartan and prazosin are in close agreement to each other, the doses reported in this study (*EXPERIMENTAL Section*) can be considered equivalent on a molar basis.

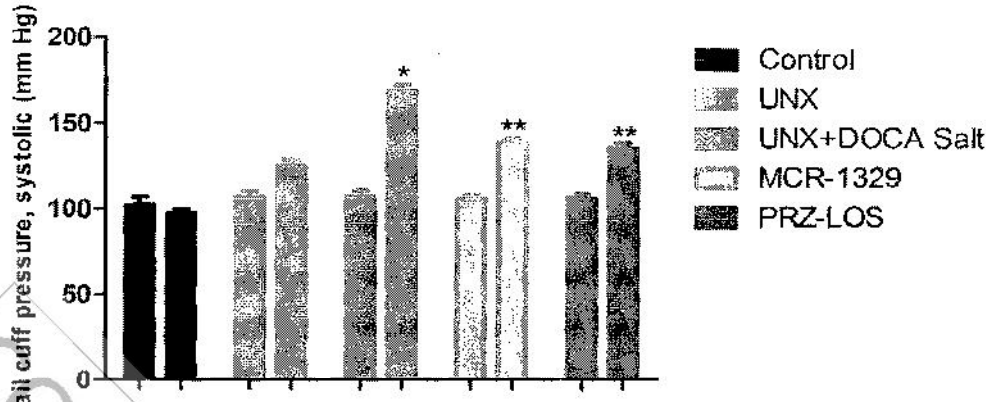


Figure 22: Figure shows the effects of mineralocorticoid induced hypertension in different groups of animals before and after induction/treatment. The figure clearly shows that all the groups are normotensive in the pre-induction phase whereas severe hypertension is evident in the UNX-DOCA Salt group. The animals treated with **MCR-1329** or a combination of prazosin and losartan were able to prevent DOCA-salt mediated hypertension in the animals. *indicates P<0.001 as compared to control group and **indicates P<0.001 as compared to the UNX-DOCA salt group.

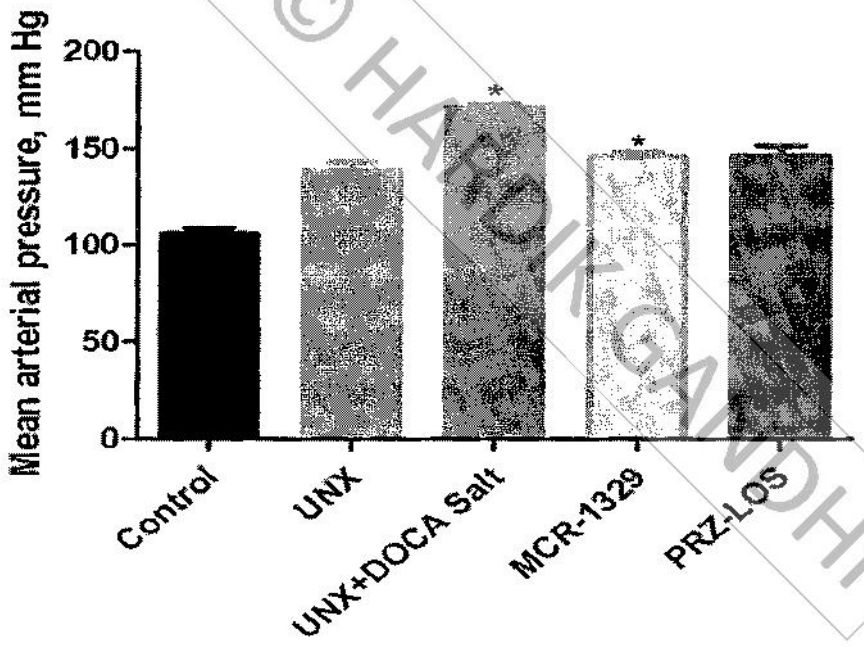


Figure 23: The columns indicate mean arterial pressures from different animals recorded at the carotid artery. It is evident from the graph that UNX-DOCA salt animals were severely hypertensive at the terminal stage of the study. Treatment with **MCR-1329** was able to ablate these destructive effects of DOCA salt and was comparable to those of standards. * indicates P<0.05 v/s control or UNX-DOCA Salt group.

***MCR-1329 halts renal damage induced by nephrectomy and mineralocorticoid***

*Renal hypertrophy*

Figure 24 indicates that UNX by itself does not lead to renal hypertrophy but mineralocorticoid induced pressure overload leads to enlargement of the renal capsule to a significant extent as suggested by Ndisang and Jadhav (2010). The unilateral renal capsule size increased nearly 2-fold suggesting the additional work done by the kidney. Moderate renal hypertrophy was also evident in the treated groups but was significantly lower as compared to the UNX-DOCA salt group. This suggested that **MCR-1329** by virtue of its effects on blood pressure and annulment of DOCA-salt mediated renal damage was able to prevent renal hypertrophy to a significant extent.

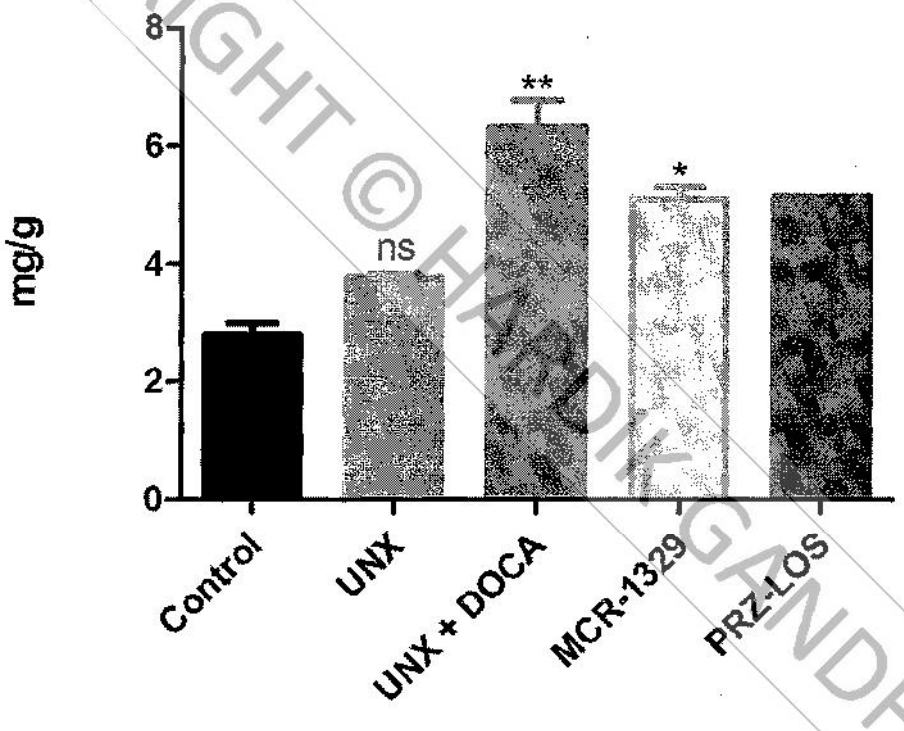


Figure 24: Figure demonstrates the ratio of kidney:body weight in different groups of animals. It is evident from the figure that UNX *per se* does not lead to kidney hypertrophy but additional overload produced by DOCA-salt causes the kidney to increase in size to compensate for GFR and other renal activities. 'ns' indicates non-significant change; *indicates $P<0.05$; **indicates $P<0.01$.

*Urinary indices*

Urinary parameters are important while studying mineralocorticoid induced hypertension since the major affected organ is the kidney. Hypertension mediated

overload leads to functional damage to the kidney which may be suggested by changes in excretion of electrolytes, creatinine, protein and glucose (Blasi *et al*, 2003; Ortmann *et al*, 2004; Artunc *et al*, 2006). Accordingly, it was decided to evaluate a battery of parameters which provide an index of renal function. It is known that mineralocorticoids like DOCA favour sodium/water retention and in turn supports excretion of potassium. In mild contrast to this finding, we found that urinary output was increased about 3-fold in DOCA-salt treated animals (82.7 ± 3.8 ml/day). This group was supplemented with 1% NaCl and 0.2% KCl in drinking water which increases the osmolarity of the drinking solution thus leading to increased volume intake and ultimately output as reported by Jia *et al* (2010) and Quigley *et al* (2009). Treated animals were also supplemented with 1% NaCl and 0.2% KCl in drinking water but the results indicated that **MCR-1329** and the standard drug therapy was able to prevent the effects of DOCA-salt on urinary output (Figure 25A). However, volume of intake was not measured as a part of this study. In concert with findings reported by others (Jia *et al*, 2010; Zhou *et al*, 1999), we also found that sodium excretion was significantly decreased (101.8 ± 6.5 mmol/lit) and potassium excretion increased (204.8 ± 8.2 mmol/lit) about 4-fold in the DOCA-salt treated group (Figure 25B, 25C). This was suggestive of increased sodium retention in the positive control group which might contribute to increased vascular volume factoring the rise in blood pressure. This data is in agreement with the findings reported by Jennings *et al* (2013), Zhou *et al* (1999) and Yemane *et al* (2010). It is important to note that **MCR-1329** was able to normalize urine (54.3 ± 4.5 ml/day) and sodium (123.1 ± 2.0 mmol/lit) output while reducing potassium excretion (158.4 ± 6.4 mmol/lit). The effects of standard therapy were found comparable to that of **MCR-1329** and were harmonious with the UNX group. The beneficial effects of **MCR-1329** in managing this condition may be attributed to its potential in controlling rise in blood pressure through antagonism of $\alpha_1$ and $AT_1$ receptors and preventing the consequent effects of angII and other endogenous vasoconstrictor molecules.

Kidneys are known to effectively excrete creatinine in the urine and block the spillage of glucose and proteins in the urine. However, when renal structure is marred due to mineralocorticoid insult reinforced by overload it is possible that creatinine secretion is reduced (Sahan-Firat *et al*, 2010) and glucose/albumin (Rhaleb *et al*, 2011; Morrison *et al*, 2005; Quigley *et al*, 2009) or other proteins may spill in the urine.

Elevated levels of glucose (26.5 ± 2.7 mg/dl/day) and albumin (41.2 ± 2.7 µg/day) were observed in the DOCA-salt group (Figure 25D, 25E). Creatinine values in urine reduced about 4-fold (Figure 25F). Normally, glucose and proteins are absent in the urine (Ndisang and Jadhav, 2010; Dawson *et al*, 2000) but DOCA-salt groups showed elevated excretion of glucose and albumin which were reduced to a significant extent by **MCR-1329** (14.5 ± 1.1 mg/dl/day glucose and 17.7 ± 1.01 µg/day albumin). Creatininuria has been suggested to be a marker of renal function (Mombelli *et al*, 2013). Creatinine secretion improved in the **MCR-1329** treated group indicating normalization of renal function.

Based on these calculations, urine osmolality and creatinine clearance were derived using formulae and the results are summarized in figure 25 alongwith other urinary indices. Urine osmolality increased by 2-fold in the DOCA-salt group (Figure 25G) which may be attributed to the excretion of electrolytes, urea and glucose in the urine as a result of damage to the Bowman's capsule reducing its filtering capability. These results contradict the findings reported by Sahan-Firat *et al* (2010) and Bae *et al* (2009) who reported a decrease in urine osmolality with DOCA-salt groups. This discrepancy in the result may be a result of reduced fluid intake in some animals from the groups. Since this parameter is derived on the basis of several other parameters it is likely that actual urine osmolality is dependent on the values of the electrolytes, proteins and glucose. A decline in glomerular filtration rate was also evident from the creatinine clearance values which were reduced to about 3-fold in the DOCA-salt group as compared to the control group. Treatment with **MCR-1329** improved the individual urinary indcies but this was not reflected on creatinine clearance (Figure 25H). As can be seen from the figure there was only modest improvement in creatinine clearance, even with standard pharmacotherapy. Urine osmolality recuperated to a certain extent following and this effect was found to outshine that of the standard combination (Figure 25G). Upon closer examination, it was observed that potassium excretion was lesser in the **MCR-1329** group which was responsible for its improved urine osmolality values. This also suggested that risk of kaluria and consequent hypokalemia is lesser with **MCR-1329**, though not a known problem with quinazoline class of compounds. The effects of DOCA-salt and **MCR-1329** upon different indices of urinary function and creatinine clearance and urine osmolality values are summarized in figure 25.

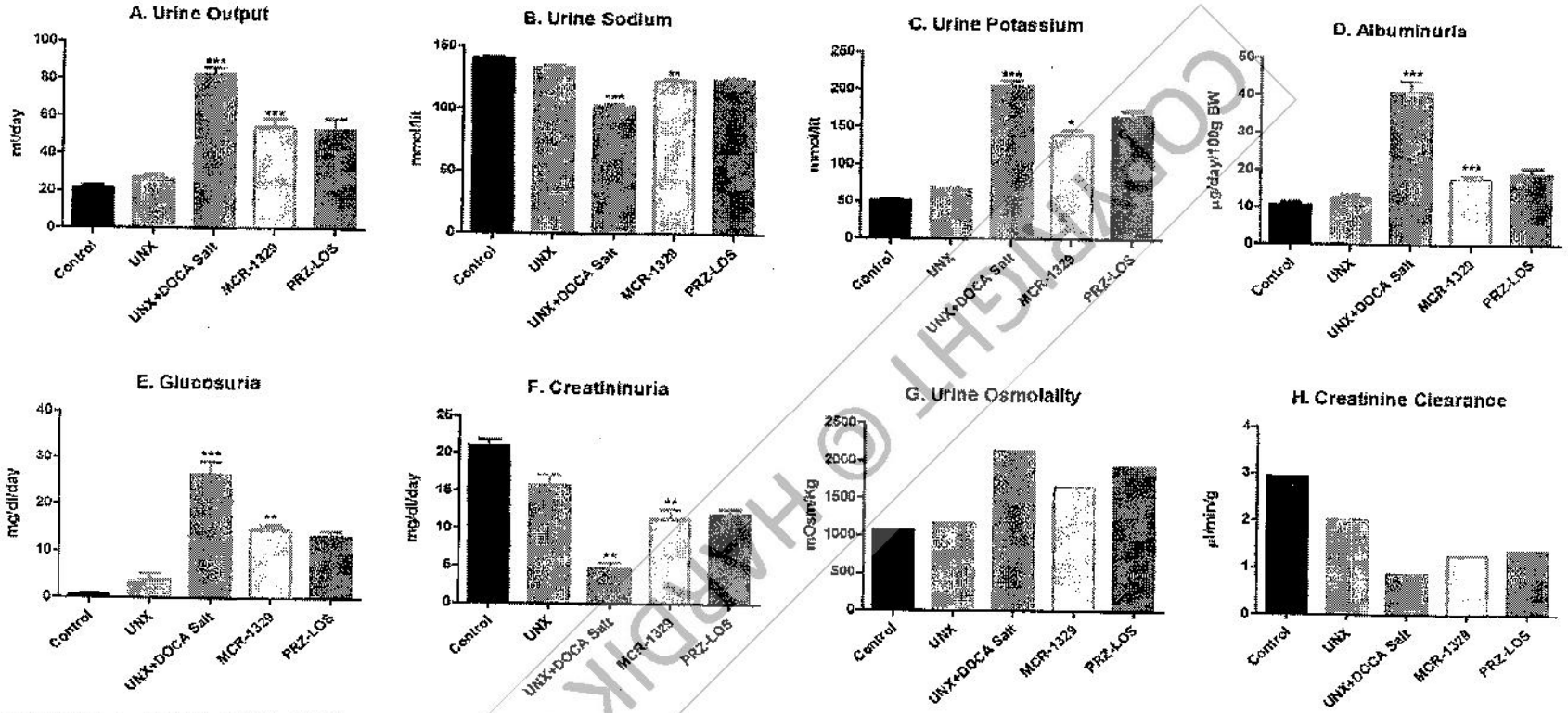


Figure 25: Effect of **MCR-1329** in UNX-DOCA salt hypertension. The figure summarizes the effect of **MCR-1329** on urinary indices like A) urine output is increased in the DOCA-salt group and normalized with **MCR-1329**, B) sodium retention is the major pharmacological effect of mineralocorticoids which is evident here. **MCR-1329** prevents retention of sodium, C) urinary potassium excretion is increased as a result of sodium retention in the DOCA-salt group. This effect was also improved with **MCR-1329** as a result of prevention of sodium retention, D, E) albuminuria and glucosuria may be considered as surrogates for glomerular function and are increased in the DOCA-salt mediated renal insult. Albuminuria reaches normalcy in the **MCR-1329** group, while glucosuria is reduced following **MCR-1329** treatment, F) DOCA-salt affected creatinine clearance is improved by **MCR-1329** therapy, G) Increased spillage of electrolytes and glucose increases urine osmolality and is prevented by **MCR-1329**, H) the unit of renal function, CrCl, is reduced in DOCA-salt group. **MCR-1329** mediated improvements are only modest. *P<0.05 as compared to UNX-DOCA salt group; **P<0.01 as compared to control or UNX-DOCA salt group; ***P<0.001 as compared to control or UNX-DOCA salt group.

***Endothelial dysfunction: role of uric acid and effect of MCR-1329 on uric acid levels***

It is known that hypertension leads to endothelial dysfunction. The major reason for this type of damage is the increase in pressure-mediated shear stress on the inner walls of arteries. This leads to gradual erosion of the endothelial layer and ultimately the effects of Ach/NO cannot be perceived (Sahan-Firat *et al*, 2010; Nunes *et al*, 2000; Jimenez *et al*, 2007). The present study dealt with evaluation of endothelial dysfunction in aortic strips from different groups of animals and comparison with sodium nitroprusside mediated relaxations. Figure 26 shows that relaxation was incomplete in strips obtained from DOCA-salt group, whereas Ach mediated complete relaxation of aortic strips from all other animals including those from the **MCR-1329** treated group. This suggested that since **MCR-1329** reins the rise in blood pressure, it might have a beneficial effect in preventing attrition of the endothelium thus maintaining the relaxant effect of endogenous vasodilators. Similar effects were observed in the standard treatment group as well.



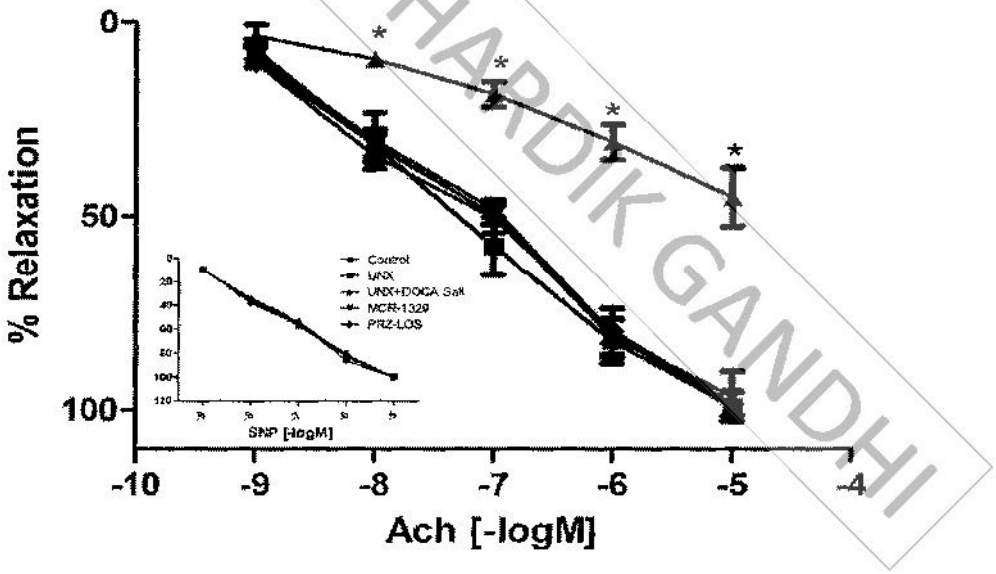


Figure 26: Cumulative concentration response curves to Ach ($10^{-9} - 10^{-5}$ M) in endothelium-intact strips precontracted with phenylephrine ($1.5 \times 10^{-6}$ M) from all the groups (n=3). Relaxation was significantly marred in strips from the DOCA-salt group. Inset shows sodium nitroprusside (SNP) mediated relaxant effects on the same strips. It is evident that SNP causes complete relaxation of the aortic strips irrespective of endothelial damage. * indicates $P<0.001$ as compared to control and **MCR-1329** group.

Uric acid has been traditionally considered as an inert metabolic product but off-late several studies have identified hyperuricemia to be a risk factor for occurrence of cardiovascular diseases (Johnson *et al*, 2003; Feig *et al*, 2008). It is not yet clear whether uric acid causes is a causative factor or a consequence of the effect of cardiovascular diseases including hypertension. Szasz and Watts (2010) evaluated the effects of uric acid on endothelial function in DOCA-salt hypertensive rats and reported that endothelial dysfunction is not predicted by uric acid levels. On the same lines we chose to evaluate the relation between endothelial dysfunction observed in the DOCA-salt group and serum uric acid levels. Contrary to the published reports it was found that uric acid levels in serum could not be correlated to any other parameter since no change was observed in the serum uric acid levels in animals from all the groups (Figure 27). One reason for such an observation would be the expression of the uric acid metabolising enzyme, uricase, in rodents which is not expressed in higher primates. This enzyme is responsible for metabolising any excess uric acid produced in the body. However, this study did not deal with estimation of allantoin which is the catabolic product of uricase activity on uric acid.



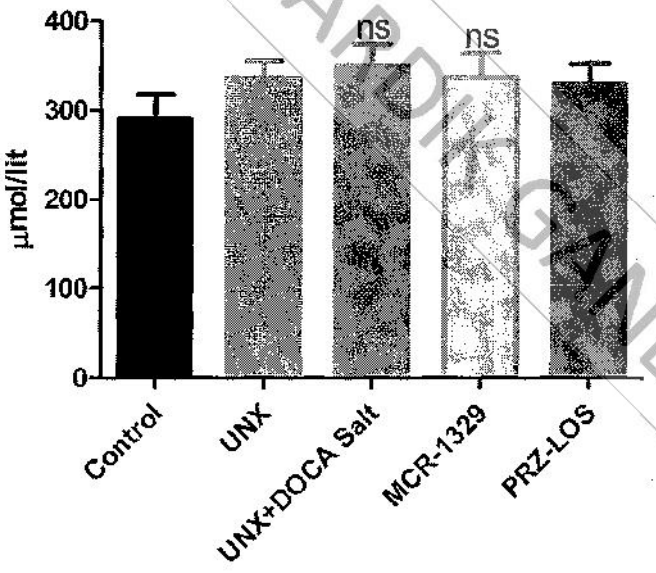


Figure 27: Uric acid levels in the serum of UNX, UNX-DOCA salt and **MCR-1329** treated animals were found to be comparable (n=5). Statistical evaluation did not show any significant difference between the groups regarding uric acid levels. ns=non significant.

***Renal histopathology***

Deposition of extracellular matrix components in the renal capsule and assessment of hypertensive damage was performed by Periodic-acid Schiff (PAS) staining (Figure 28) as described by Kiernan *et al* (1999). PAS staining is typically used to identify carbohydrate macromolecules like glycogen, proteoglycans and glycolipids deposited as matrix components in tissues. In a controlled reaction, the vicinal diols of the sugars present in these carbohydrates undergo oxidation with periodic acid and result in the formation of a pair of aldehydes. These aldehydes react with the Schiff reagent to give purple/magenta coloured complexes (Kiernan *et al*, 1999). Since nuclei are not stained with this stain, hematoxylin is used as a basic counter stain to visualise the nuclei. This technique is also utilised for the visualization of renal histoarchitecture. Several studies have reported the renal damage occurring in rats following DOCA-salt administration. It has been shown that mineralocorticoid and salt administration leads to cortical damage, glomerulosclerosis and tubulointerstitial damage (Blasi *et al*, 2003; Kim *et al*, 1994; Peng *et al*, 2001). There is damage to renal blood vessels resulting in luminal obliteration and blockade of blood flow in respective regions supplied by those blood vessels (Blasi *et al*, 2003; Lezin *et al*, 1999; Wang & Wang, 2009). Renal sections from the DOCA-salt group of the present study showed several PAS-positive sections indicating extracellular matrix deposition in the form of glycans. These were identified by dark purple regions in the sections. Glomerular damage was also evident and it was observed that Bowman's capsule had lost its normal morphology with the capillary tufts losing their normal formation and touching the glomerular walls (Figure 28E). Thickening of cortical cells (Figure 28F) due to matrix deposition and presence of hyaline casts were evident (Figure 28E). Glomerular basement membrane damage was identified by an absence of clear demarcation between the tufts and Bowman's capsule. Recuperation of these damages was observed in the treatment groups. A normal cortical area was observed in renal sections from **MCR-1329** and standard groups. PAS-positive areas were observed at the bowman's capsular walls in the **MCR-1329** group (Figure 28H) and near the cortical cells in the standard group (Figure 28J). The UNX group did not show any major pathological changes except for a few PAS-positve areas. The control group sections remained PAS-negative.

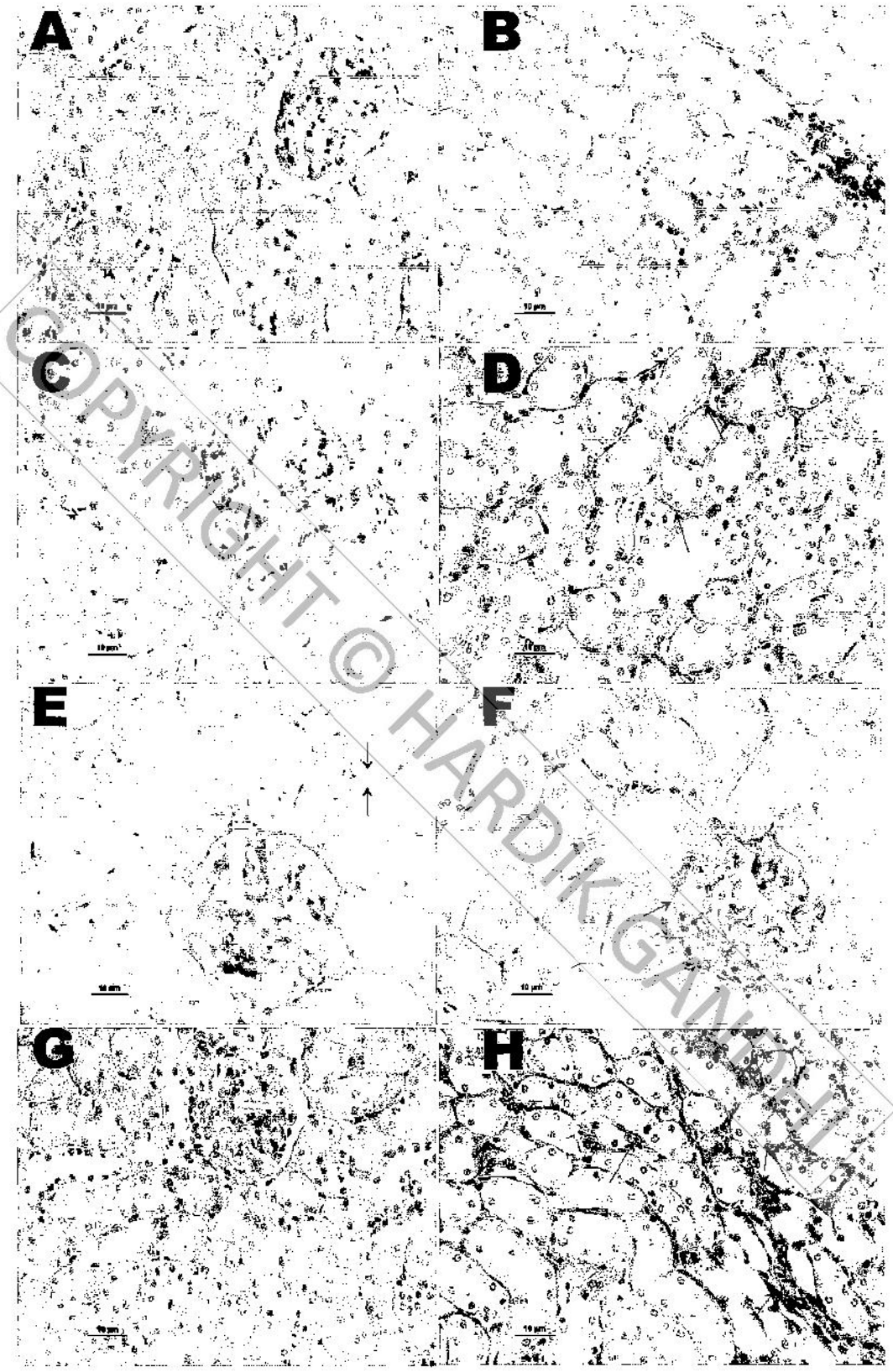

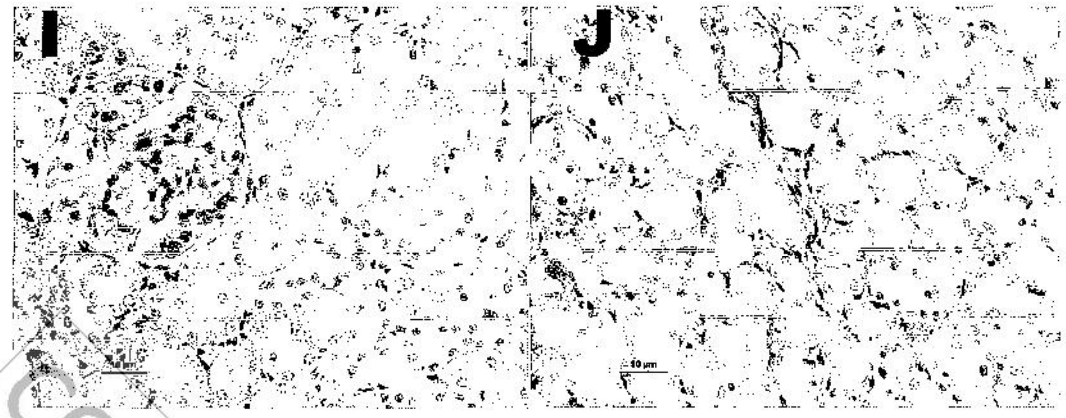


Figure 28: Light micrographs representing renal histology of different groups (Periodic acid schiff stain, 40X, bars represent 10μm). Control group (A, B), UNX (C, D), DOCA-salt (E, F), DOCA-salt + **MCR-1329** (G, H) and DOCA-salt + standard (I, J). While figures A-B virtually show no pathological changes, E-F are indicative of hypertensive renal damage in the cortical region as well as glomeruli. Derangements in the cortical cells and capillary tufts are evident. In contrast, figures G-J are relatively protected from damage and cortical cells appear normal, however, reduction in the space between capillary tufts and glomerular inner walls are still evident at the terminal stage.



## CELL CULTURE STUDIES

### *Cytotoxicity assay*

Before initiating the cell-signaling studies, it was important to determine the extent of cytotoxicity produced by **MCR-1329** on the cell line utilised. If the cells produce major cytotoxicity at concentrations used for the study, then cell signaling studies cannot be performed as treatment might lead to death of cells. Accordingly, cytotoxic potential of **MCR-1329** was evaluated on the rat aortic smooth muscle cell line by the MTT assay. The results of the study are shown in figure 29.

### *Cell signaling studies*

The $PI_3K$ pathway in VSMCs is important in relation to proliferation, mitogenesis, cell cycle progression and a range of cellular processes (Shigematsu *et al*, 2000; Katso *et al*, 2001). Its role has also been implicated in the pathogenesis of hypertension (Yang and Raizada, 1999; Quignard *et al*, 2001; Carnevale *et al*, 2012b). $PI_3K$ is directly involved in vascular remodelling and proliferation of major and minor blood vessels (Saward and Zahradka, 1997). There are several downstream targets of

$PI_3K$ like PDK-1 (Phosphoinositide-dependent Kinase 1), Akt and $p70^{S6K}$ (p70 ribosomal protein S6 kinase) among others.

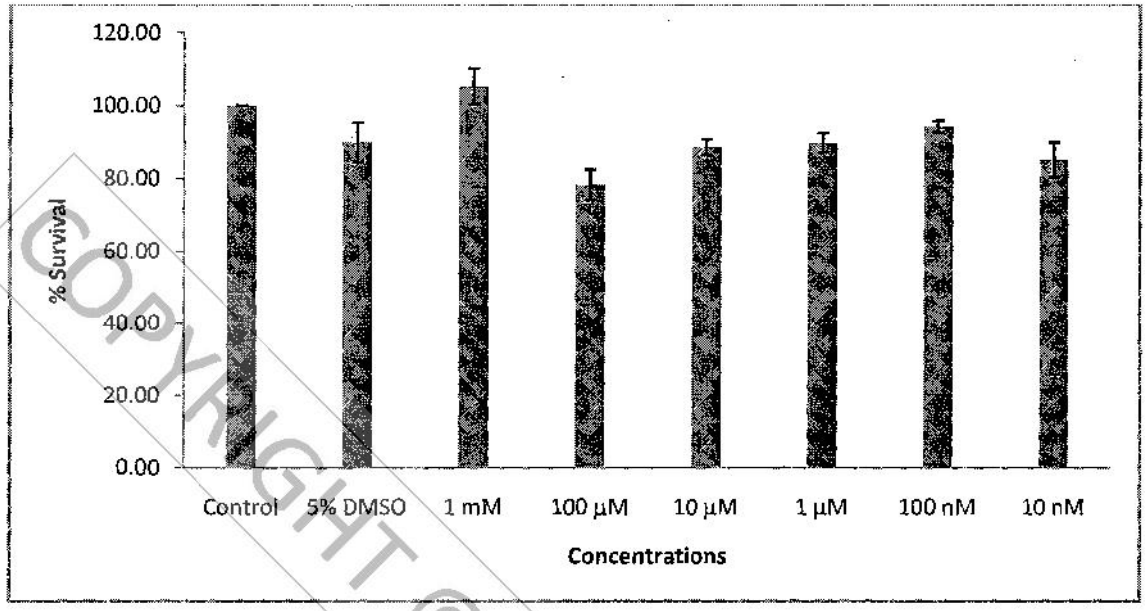


Figure 29: Survival of cells post-incubation with different concentrations of **MCR-1329**, vehicle and control cells are shown (n=6). Survival was found to be >80% at most of the concentrations suggesting that **MCR-1329** is not cytotoxic upto a concentration of 1mM. Statistical analysis did not find any significant difference between the groups.



Of these, Akt is one of the major downstream targets (Quignard *et al*, 2001). $PI_3K$ mediated activation of Akt is induced through phosphorylation of Akt at Thr-308 (Alessi *et al*, 1997) however, some researchers have also indicated phosphorylation at Ser-473 (Toker and Newton, 2000; Atwell *et al*, 2000). Several lines of research indicate that $PI_3K$ signaling activated through hypertensive afferents like angII and α1 agonists involve Akt as the major downstream molecule (Takahashi *et al*, 1999b; Dugourd *et al*, 2003). It has been shown that angII, norepinephrine and phenylephrine are able to increase the phosphorylation of Akt at Thr-308 and/or Ser-473 (Li and Malik, 2005b). In addition, antagonists of $AT_1$ and $\alpha_1$ receptors are able to prevent or reduce agonist-mediated Akt-phosphorylation (Dugourd *et al*, 2003). All such studies have utilised either wortmannin or LY-294002, known inhibitors of $PI_3K$, to show that agonist-mediated Akt-phosphorylation is mediated through $PI_3K$ signaling (Kippenberger et al, 2005; Dugourd *et al*, 2003). Based on these evidences, it was decided to evaluate **MCR-1329** for its potential to block agonist-mediated Akt-

phosphorylation. Since Ser-473 is debatable (Toker and Newton, 2000; Atwell *et al*, 2000), it was chosen to evaluate the Thr-308 phosphorylation of Akt using flow cytometry. Results indicated that both angII and phenylephrine were able to induce Akt-phosphorylation to a significant extent in rat aortic smooth muscle cells. Figure 30 shows the controls indicating that cell treatments and the 2° antibody by itself do not show fluorescence as such, but as shown in Figure 31A, phenylephrine causes significant increase in the fluorescence which is a result of Akt-phosphorylation at Thr-308 and consequent binding of the antibodies (indicated by the presence of the P3 population in the histogram).

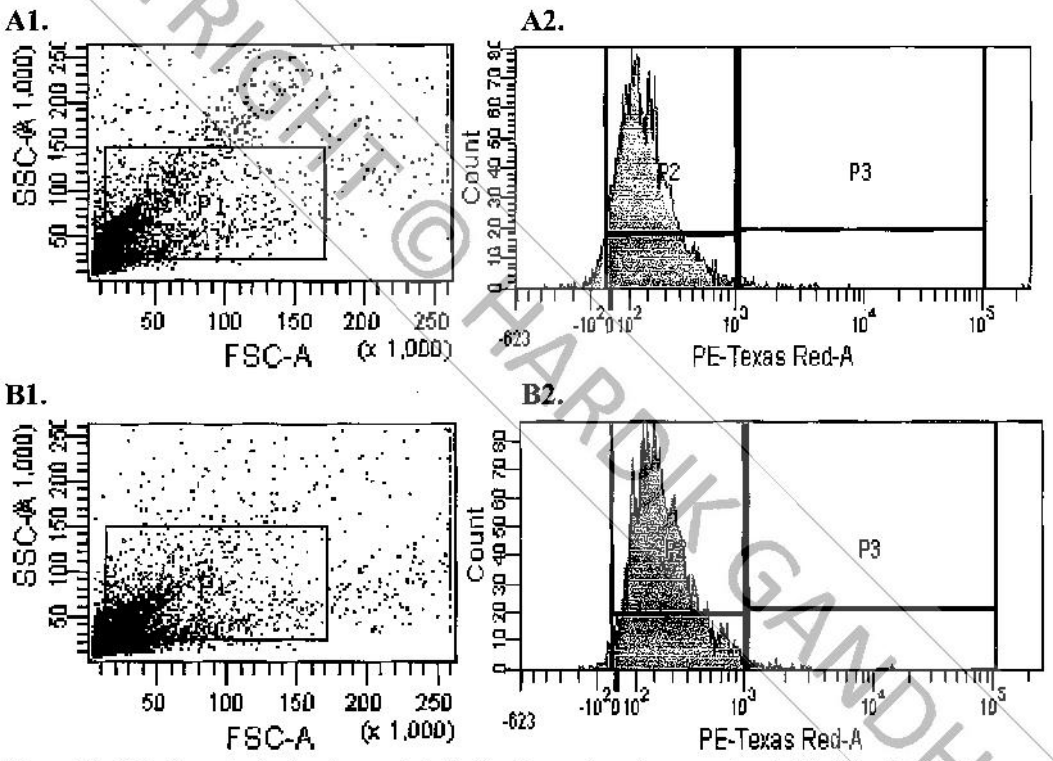


Figure 30: This figure indicates the controls in the flow cytometry experiment. Unstained cells shown no deviation from the parent population (A) and treatment with only 2° antibody did not show any major shift towards the P3 population (B) suggesting that washing efficiency and dilutions are optimal.

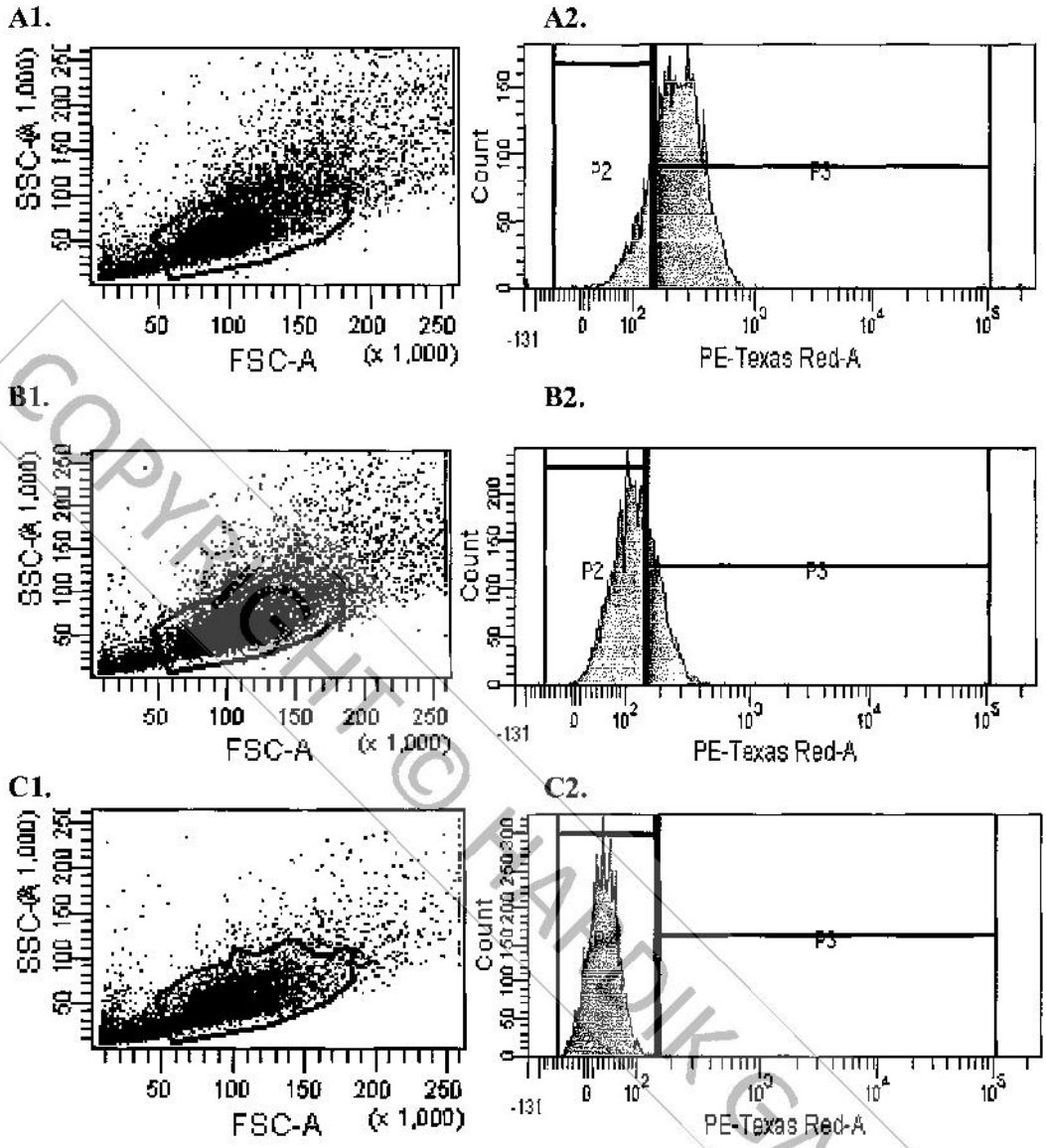


Figure 31: The scatter obtained from flow cytometry and corresponding histograms are shown here. P1 is the entire population gated from 10000 events. The figures represent different treatments: A, Stim1 (phenylephrine); B, Stim1 + **MCR-1329**; C, Stim1 + **MCR-1329** + LY294002

Similar results were obtained when angII was used to stimulate the cells (Figure 32A). Treatment with **MCR-1329** showed a 40-50% reduction in Akt-phosphorylation (Figures 31B and 32B). LY294002 is a selective inhibitor of $PI_3K$ isoforms, comparable to wortmannin (Dugourd *et al,* 2003; Yang and Raizada, 1999). When LY294002 was used in conjunction with **MCR-1329**, it was observed that Akt-phosphorylation was completely blocked (Figures 31C and 32C) suggesting that **MCR-1329** prevents PI3K mediated Akt-phosphorylation. These results are in conjunction with previous studies

showing the role of AT1 or α1 antagonists in preventing PI3K-mediated activation of Akt. Dugourd *et al* (2003) and Yang and Raizada (1999) respectively showed the effect of irbesartan and losartan in preventing Akt-phosphorylation. Wang *et al* (2005), were able to show that prazosin prevents phenylephrine-mediated activation of Akt. These studies also showed that agonist-mediated effects were doctored by $PI_3K$ as suggested through complete inhibition when LY294002 was employed.

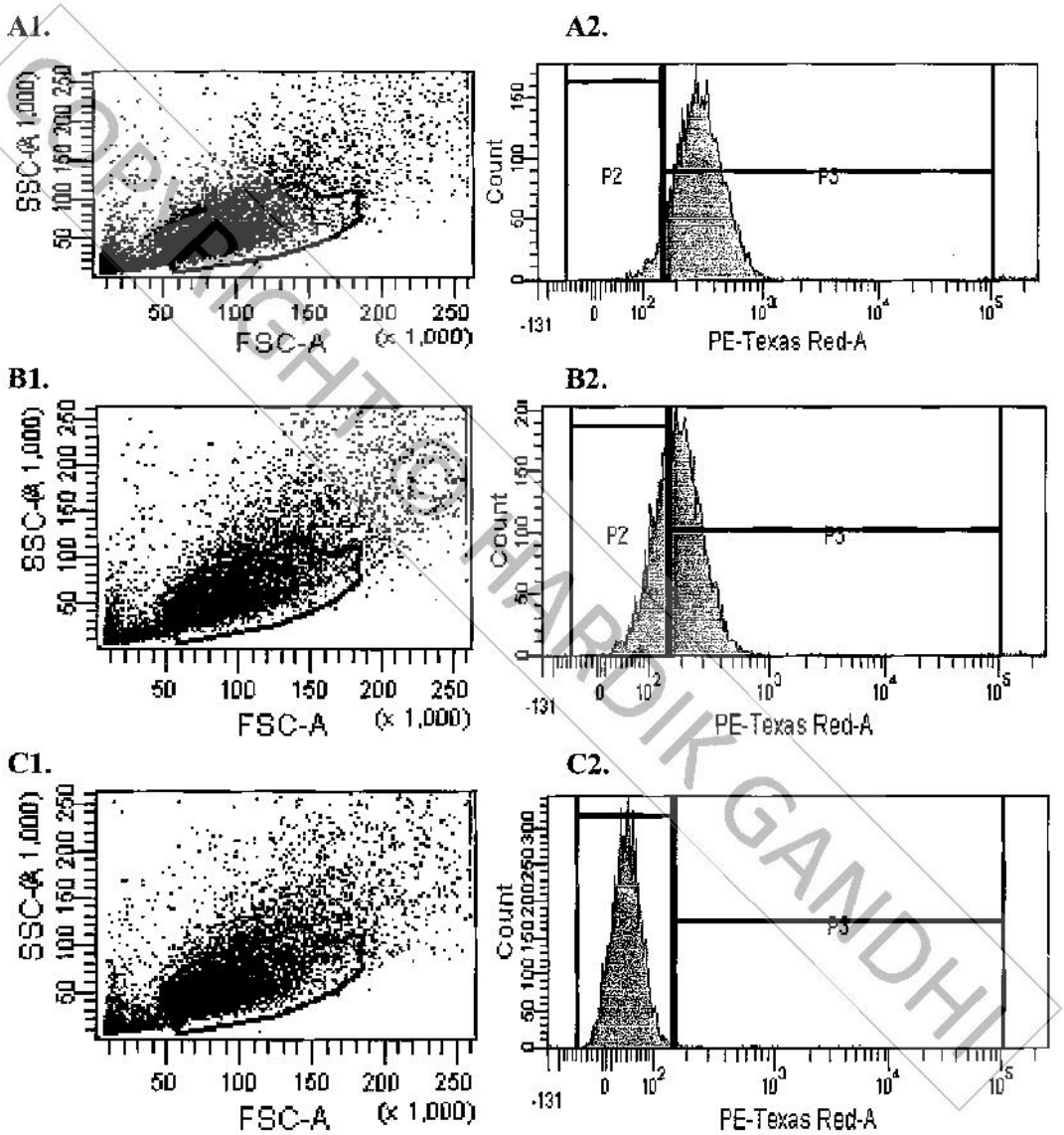


Figure 32: The scatter obtained from flow cytometry and corresponding histograms are shown here. P1 is the entire population gated from 10000 events. The figures represent different treatments: A, Stim2 (AngII); B, Stim2 + **MCR-1329**; C, Stim2 + **MCR-1329** + LY294002

Based on these results it was concluded that the beneficial effects of **MCR-1329** are, in part, mediated through inhibition of $PI_3K$-mediated Akt-phosphorylation. The quantitative results are summarized in Table 16.

**Table16: Quantitative summary of flow cytometry data**

| Sr. No. | Treatment | P1 population (no. of cells) | P2 (% of P1) | P3 (% of P1) |
|---|---|---|---|---|
| **CONTROLS** | | | | |
| 1 | Control (Unstained) | 5134 | 96.9 | 1.2 |
| 2 | Secondary Antibody | 5456 | 94.0 | 1.4 |
| **PHENYLEPHRINE STIMULUS** | | | | |
| 3 | Stim1 (PE) | 5338 | 16.8 | 77.6 |
| 4 | Stim1 + **MCR-1329** | 5667 | 66.8 | 25.3 |
| 5 | Stim1 + **MCR-1329** + LY294002 | 4855 | 99.8 | 0.2 |
| **ANGIOTENSIN II STIMULUS** | | | | |
| 6 | Stim2(AngII) | 4571 | 5.4 | 91.2 |
| 7 | Stim2 + **MCR-1329** | 5543 | 32.9 | 59.2 |
| 8 | Stim2 + **MCR-1329** + LY294002 | 5614 | 99.3 | 0.5 |

On the basis of the present findings, it may be said that receptor-mediated activation of $PI_3K$ and subsequent AKt-phosphorylation may be the key events related to the development of hypertension and that antagonism of $\alpha_1$ and angII receptors can certainly abrogate hypertension mediated through these mechanisms.

# RESULTS
# &
# DISCUSSION

# RESULTS & DISCUSSION

## SCREENING OF POTENTIAL ACAT INHIBITORS

The aim of this study was the screening of ACAT inhibitors. The screening process required that an *in vivo* or *in vitro* enzymatic reaction should take place so that the test compounds could be added/administered at appropriate time-points to evaluate their inhibition potential. It was chosen to utilize the *in vitro* cell-free ACAT enzyme based assay for evaluation of the test compounds since this assay was relatively simple, many test compounds could be studied simultaneously and the methods for determining completeness of the reaction were known, *i.e.* through quantification of cholesteryl esters formed in the reaction mixture. Based on a review of literature, it was known that radiometric scanning was the most commonly employed technique for the detection of cholesteryl esters. Researchers most commonly used radiolabeled substrates like $C^{14}$-oleoyl CoA, $H^{3}$-cholesterol or $C^{14}$-cholesterol. This resulted in formation of radiolabeled products having the respective labelled atoms in their structure. This radioactivity could be quantified simply using either a liquid scintillation counter or through radiometric scanning (Erickson *et al*, 1980b; Chang *et al*, 1998; Temel *et al*, 2003). One major caveat in these studies was that it required separation of the labelled products from the reactants and substrates otherwise the radioactivity measurements would give false negatives since the entire substrate might not be used up in the reaction. As an alternative, different research groups utilized thin layer chromatography as a means of separating the products formed as a result of the catalytic reaction, sprayed the plates with iodine vapours to visualize the cholesteryl ester bands and then scrapped the regions from the silica plates to process them for liquid scintillation based quantification. This method was tedious and employed radiometry as a technique for quantification (Largis *et al*, 1989; de Medina *et al*, 2004; Lada *et al*, 2004; Mizoguchi *et al*, 2004). Handling of radiometric reagents is a complex issue with lot of precautions and specialized areas and training being needed for handling such material. Apart from this, disposal of radiometric waste is another global concern. In lieu of this, it was decided to develop a non-radiometric, planar chromatography-based technique which could allow densitometric quantification of cholesteryl esters.

**STANDARDIZATION OF ACAT ASSAY**

This assay is a cell-free enzyme-based *in vitro* assay where substrates are added to the reaction mixture, enzyme and the test compounds are incubated previously and the reaction is allowed to proceed for a finite time at the end of which the products are extracted from the reaction mixture and quantified. Several reports have shown different modifications of the ACAT assay procedure (Tomoda *et al*, 1992; Cases *et al*, 1998; Lada *et al*, 2003). Accordingly, it was decided to standardize the reaction based on the available literature. As shown in the '*EXPERIMENTAL*' section, the reaction utilizes phosphate buffer, bovine serum albumin (BSA), a source of ACAT enzymes and cholesterol & oleoyl CoA as substrates. Different buffers have been indicated as a reaction medium for the ACAT assay like 10 mM Tris-buffer, 50 mM Tris-sucrose buffer, 0.154 M potassium phosphate buffer or 0.1 M potassium phosphate buffer (Chang *et al*, 1993; Temel *et al*, 2003; Liu *et al*, 2005). However, all the buffers are known to have good buffer-capacity and allow maintenance of normal tonicity and *p*H (~7.4) at 37 °C. Assay components are known to remain stable in these buffers; preparation of all the buffers is relatively simple and any buffer does not offer advantage over the other. Hence, 0.1 M potassium phosphate buffer was arbitrarily chosen for further protocols. BSA is added to prevent the small quantities of the enzyme being used in the assay from being lost by adhering to the reaction vessel walls. Alternatives to the use of BSA are egg albumin and fetal bovine serum (FBS). However, the purity of BSA is higher as compared to these reagents. Additionally, unnecessary enzyme and test compound binding may occur with FBS which would not be acceptable. Some researchers have also suggested removal of BSA altogether from the reaction mixture to reduce non-specific binding of test components (Llaverias *et al*, 2003) but in the present study no difference was observed in the data of standard inhibitor when BSA was present or absent in the reaction media. Microsomal ACAT protein was used as the source of the enzyme to catalyze the esterification process. Alternatively, S9 fraction of the liver homogenate (supernatant of a liver homogenate centrifuged at 9000×*g* for 20 mins) may also be utilized as a source of the enzyme. This fraction may be lyophilized and used as a crude enzyme source after protein quantification. However, presence of a lot of non-specific and uncharacterized substances in this fraction is liable to give false-positive and false-negative data. Another alternative is to use the purified enzyme obtained from recombinant sources or chemically-synthesized in commercial labs through peptide synthesis. However, such

sources are rarely available and if at all, are extremely costly and do not offer rationale for a screening process (Cho *et al*, 2003). Hence, microsomal ACAT was utilized for all assays in this study. Cholesterol is a hydrophobic molecule and is not soluble in aqueous solvents. Use of organic solvents in the assay may negatively affect enzyme activity and hence cholesterol was solubilized using 45% w/v hydroxypropyl β-cyclodextrin since this excipient has been reported not to affect the activity of biological enzymes (Karuppiah *et al*, 1993). The bulky and hydrophobic cholesterol is easily lodged inside the cyclodextrin cavity and thus becomes available for an aqueous medium. Cholesteryl oleate is by far, the most abundant cholesteryl ester in any mammalian cell and hence it was decided to use oleoyl CoA as the other substrate (Liu *et al*, 2005). Alternatives to oleoyl CoA include palmitoyl- and stearoyl CoA (Liu *et al*, 2005). After optimization of the assay reagents and their concentrations, it was important to extract the reaction products. Since cholesteryl esters are freely soluble in organic solvents like chloroform and methanol, a mixture of both in a ratio of 2:1 was utilized for the extraction purpose. However, the experimental trials indicated that volume of the extraction solvents are critical for achieving a reliable extraction of the product formed. When equal volumes of extraction solvent were used (*i.e.* equal to the volume of reaction mixture), no spot of the ester was obtained on TLC. Similar issue remained for upto 2-3 volumes of the extraction solvent even when multiple extractions were performed. It was realized that extraction of the cholesteryl esters might not be complete with such lower volumes and when 6-8 volumes of extraction solvent was employed for extraction, appropriate spot were obtained. When 6-8 volumes were utilized for extraction, the extract was concentrated and dried under $N_2$ vapors. The dried extract of cholesteryl esters were reconstituted in 500µl mixture of chloroform: methanol (2:1) before application to TLC plates.



**OPTIMIZATION OF CHROMATOGRAPHIC CONDITIONS**

Optimization studies were carried out using standard solution of cholesteryl oleate, which was the analyte of interest in the present study. Based on the literature available for separation of cholesteryl esters like cholesteryl oleate and cholesteryl palmitate, several mobile phases were tried to obtain a good resolution of cholesteryl oleate (Largis *et al*, 1989; de Medina *et al*, 2004; Lada *et al*, 2004; Mizoguchi *et al*, 2004). The basic idea was to find a mobile phase which showed good resolution of cholesteryl oleate from other reagents like cholesterol and oleoyl CoA, had an $R_f$ value

between 0.2-0.8, showed no tailing or fronting abnormalities and did not produce unnecessary charring or pigmentation of the samples before sample derivatization and quantification is performed. Different mobile phases, involving combinations of hexane, ether, acetic acid and ethyl acetate (Kupke and Zeugner, 1978; Touchstone, 1995, de Medina *et al*, 2004), evaluated for resolving cholesteryl oleate, are enlisted in table 3 below:

**Table 3: Different mobile phase systems for resolution of cholesteryl oleate**

| Sr. No. | Mobile Phase Composition (ratio; v/v/v) | Comments |
|---|---|---|
| 1. | *n*-Hexane: diethyl ether: acetic acid (70: 30: 1) | $R_f$ is greater than 0.9; resolution of assay products is inadequate; tailing is another issue |
| 2. | *n*-Hexane: diethyl ether: acetic acid (50: 50: 1) | $R_f$ value too low; not resolved from cholesterol |
| 3. | *n*-Hexane: diethyl ether (70: 30) | $R_f$ is greater than 0.9 |
| 4. | *n*-Hexane: diethyl ether (80: 20) | $R_f$ is greater than 0.9 |
| 5. | *n*-Hexane: diethyl ether (90: 10) | $R_f$ is $\geq$ 0.9 |
| 6. | *n*-Hexane: diethyl ether (94: 6) | Optimal $R_f$ (0.6-0.7) |
| 7. | *n*-Hexane: diethyl ether (95: 5) | Optimal $R_f$ (~ 0.6) |
| 8. | Petroleum ether: diethyl ether: acetic acid (70: 30: 0.5) | Tailing is observed in samples |
| 9. | *n*-Hexane: ethyl acetate (90: 10) | $R_f$ is $\geq$ 0.8 |
| 10. | *n*-Hexane: ethyl acetate (95: 5) | $R_f$ is greater than 0.9 |
| 11. | *n*-Hexane: ethyl acetate (93: 7) | Tailing and bizarre run, $R_f$ is greater than 0.9 |
| 12. | Diethyl ether: petroleum ether (95: 5) | Tailing is observed in samples |
| **13.** | ***n*-Hexane: diethyl ether: acetic acid (90: 10: 1)** | **Optimal $R_f$ of analyte (~ 0.6) and very low $R_f$ for substrate cholesterol** |

The mobile phase optimized to *n*-hexane: diethyl ether: glacial acetic acid (90:10:1, v/v/v) gave a well-resolved peak with Gaussian symmetry ($R_f$ = 0.59 ± 0.02,

Figure 4) and the same was used for further analysis. No immiscibility issues were observed with the chosen composition of mobile phase. Another advantage of this composition of mobile phase is that the $R_f$ value of the substrate cholesterol is very low (0.05) hence it does not interfere with the detection of the cholesteryl oleate even if it is added in excess amount. Chamber saturation time was found to strongly affect the $R_f$ value of cholesteryl oleate and was therefore optimized to be 30 minutes. Apart from the chamber saturation time, it was also observed that volume of mobile phase in the twin trough chamber was critical to the optimal $R_f$ of the analyte. While higher volumes led to washing of the applied samples, very low volumes led to increased run time that affected $R_f$ values. After trial and errors, the volume of mobile phase was decided to be 36-40 ml so that it got distributed equally to both the troughs and each trough therefore contained 18-20 ml of the mobile phase. Since the mobile phase contained highly volatile organic solvents, it was freshly prepared for each run. After several experiments it was concluded that the chosen mobile phase required nearly 18 minutes of run time. The effect of temperature and humidity was also considered for the experiment and at all the times the experiments were conducted at 25± 2 °C at an ambient relative humidity of 40-60%. Ambient temperature was not considered for the experiments since temperature and humidity variations at ambient conditions could affect the mobile phase composition and hence quantification of the analyte. The analyte of interest, cholesteryl oleate, could be analysed using an ultraviolet wavelength of 205 nm but at such low wavelengths background signal and noise might result in errors in the analysis and it is routinely necessary to derivatize the analyte spots before they can be detected. In the preliminary stages of the study, iodine vapors were used for detection and scanning of the spots of cholesteryl oleate (de Medina *et al*, 2004). Use of iodine is convenient and allows detection of the samples in visible light but iodine being volatile in nature, errors occurred in the detection of samples due to a gradual decrease in intensity of the bands. Another alternative for detection purpose was a combination of 50 mM $MnCl_2$ and 6% $H_2SO_4$ (Musanti *et al*, 1996) which resulted in production of $MnSO_4$ *in situ*. However, when this detection reagent was utilized, the intensity of the bands was very less and heating of the TLC plates at 120 °C for 15-20 mins after derivatization did not result in an increase in intensity. Henceforth, anisaldehyde-sulphuric acid reagent was used for spot identification and detection. This reagent was found to give an intense purple color with cholesteryl oleate after heating (120 °C for 8 mins) and the intensity also remained stable over the period of analysis.

## METHOD VALIDATION

*Linearity and Range*

Least square regression method was used for calculation of correlation coefficient, slope and intercepts. The calibration curve was found to be linear in the range of 100-500 ng/band. The linearity of the calibration curves was validated by a value of correlation coefficient closer to unity. Each reading was an average of 3 determinations (Figures 5, Table 4).



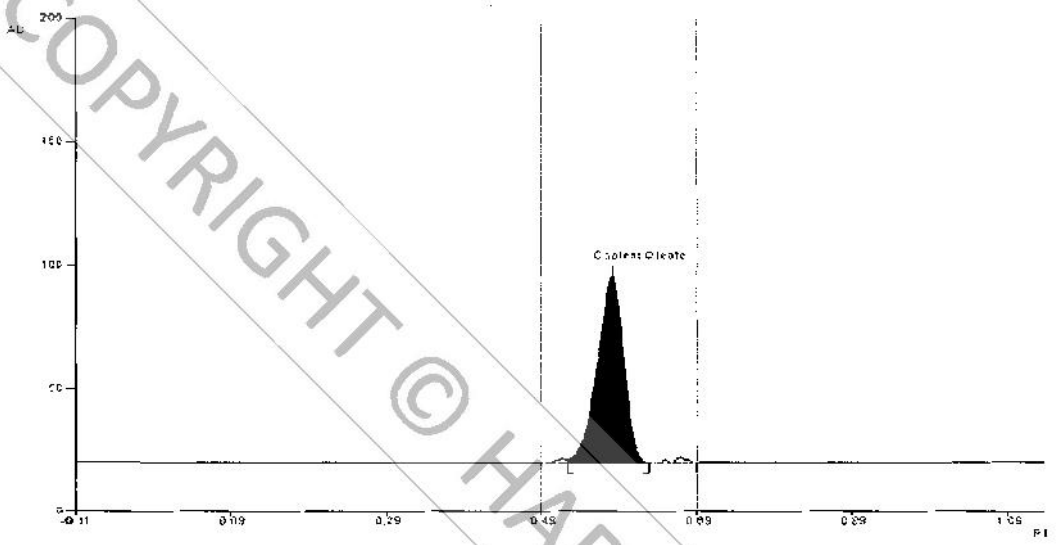


Figure 4: A typical chromatogram of cholesteryl oleate. This representative chromatogram depicts the $R_f$ value of standard cholesteryl oleate (~ 0.59) obtained upon using the current method. A concentration of 400 ng/band was utilized to obtain this chromatogram.

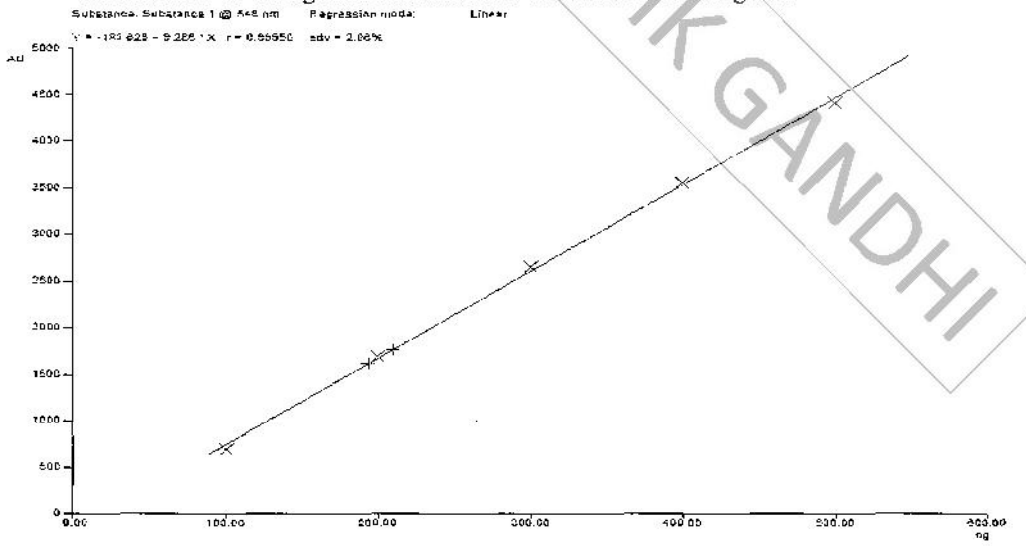


Figure 5: A typical regression curve obtained for standard and test samples of cholesteryl oleate. Coefficient of correlation closely approaches unity and quantity of cholesteryl oleate in the test samples also falls on the linearity curve.

*Limit of detection (LOD) and limit of quantification (LOQ)*

LOD and LOQ were calculated as per the formulae mentioned in the materials & methods section. Based on the formulae, LOD and LOQ for cholesteryl oleate were found to be 6.45 ng and 19.54 ng respectively (Table 4). However, by experimentation LOD and LOQ were found to be 10 ng and 25 ng respectively. Such low values of LOD and LOQ suggest that the method is adequately sensitive for analytical purposes.

*Precision and Accuracy*

The repeatability of sample application and measurement of concentrations based on peak areas were expressed in terms of % RSD and are depicted in table 5. Table 5 shows the intra- and inter-day variations of cholesteryl oleate at three different levels (200, 300 and 400 ng/band). The proposed method afforded a recovery within the range of 96.88-103.01% suggesting that the method is accurate and can be used for the quantification of cholesteryl oleate.

*Specificity*

The method was found to be robust as no interfering substances were found near the $R_f$ value of cholesteryl oleate when the standard and sample lanes were compared. Further, there was no difference between the peak of standard cholesteryl oleate and the one obtained from the sample as determined by peak start, peak apex and peak end positions. An overlay of chromatograms from standard and samples of cholesteryl oleate is shown in figure 6. Further to this, it was observed that the biological matrix does not lead to any interference *per se* (Figure 7).

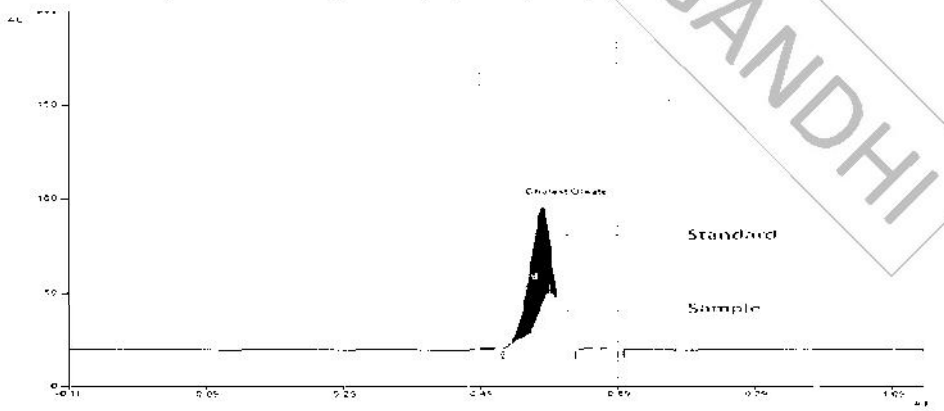


Figure 6: An overlay of the peaks obtained from standard and samples of cholesteryl oleate. This figure shows that the relative retention of standard cholesteryl oleate and from analyte samples remains the same. It may also be observed that no interference could be found in the analyte detection range.

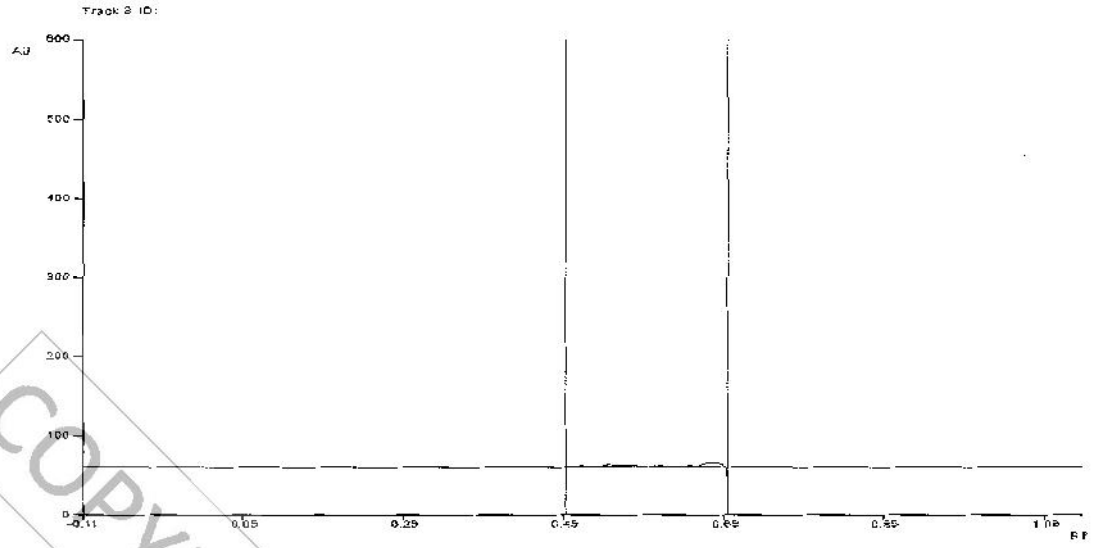


Figure 7: No peaks were found at the sample Rf when blank matrix was utilized for spotting

*Robustness*

The SD of peak areas was calculated for each determined parameter and %RSD was calculated. The values of %RSD (as shown in table 6) indicate that the method is robust and minor changes in experimental conditions do not affect analysis of cholesteryl oleate.

*Validation of the method in plasma samples*

The results of the validation of the method are shown in table 13. The % recovery of this method was found to be between 101.05-105.87 % suggesting the accuracy of the method. The low RSD values (Table 7) indicate that the method may be applied to the estimation of cholesteryl esters in pathological samples.

**Table 4: Linear regression data of calibration curves[†1]**

| Range (ng/band) | r ± SD | Slope ± SD | Intercept ± SD | LOD (ng/band) | LOQ (ng/band) |
|---|---|---|---|---|---|
| 100-500 | 0.9996 ± 0.0002 | 10.295 ± 0.95 | 205.703 ± 0.63 | 6.45 | 19.54 |

r, correlation coefficient; † n = 6

**Table 5: Precision and Recovery[2]**

| Nominal Concentration (ng/band) | Intra-Day | | | Inter-Day | | |
|---|---|---|---|---|---|---|
| | Conc. Found (ng/band) | Accuracy (%recovery) | Precision (%RSD) | Conc. Found (ng/band) | Accuracy (%recovery) | Precision (%RSD) |
| 200 ng | 193.76 ± 1.19 | 96.88 ± 0.59 | 0.61% | 198.28 ± 2.61 | 99.14 ± 1.31 | 1.32% |
| 300 ng | 309.04 ± 3.73 | 103.01 ± 1.24 | 1.21% | 302.02 ± 2.07 | 100.67 ± 0.69 | 0.68% |
| 400 ng | 401.94 ± 4.77 | 100.49 ± 1.19 | 1.19% | 394.99 ± 3.19 | 98.75 ± 0.80 | 0.80% |

[1] Linear regression data for cholesteryl oleate in the range of 100-500 ng/band
[2] Intra- and inter-day precision of the HPTLC method and recovery studies

**Table 6: Robustness of the method**[3]

| Parameter | Mean peak area | SD of peak area | %RSD |
|---|---|---|---|
| Mobile phase composition | 4765.20 | 51.10 | 1.07 |
| Mobile phase volume | 4251.00 | 46.43 | 1.02 |
| Temperature | 4555.90 | 55.47 | 1.30 |

**Table 7: Validation using plasma samples**[4]

| Nominal Concentration (ng/band) | Intra-Day | | | Inter-Day | | |
|---|---|---|---|---|---|---|
| | Conc. Found (ng/band) | Accuracy (%recovery) | Precision (%RSD) | Conc. Found (ng/band) | Accuracy (%recovery) | Precision (%RSD) |
| 200 ng | 211.35 ± 3.43 | 105.67 ± 1.71 | 1.62% | 207.66 ± 3.24 | 103.83 ± 1.62 | 1.56% |
| 300 ng | 317.61 ± 3.02 | 105.87 ± 1.01 | 0.95% | 316.82 ± 5.43 | 105.61 ± 1.81 | 1.72% |
| 400 ng | 406.84 ± 4.28 | 101.71 ± 1.09 | 1.05% | 404.20 ± 7.90 | 101.05 ± 1.97 | 1.96% |

[3] Robustness was evaluated by utilizing 3 different compositions of mobile phase. Total volume of the mobile phase and temperature of analysis were varied by ± 5%.

[4] Validation of the estimation method in pooled plasma samples. Results indicate the accuracy and precision of the method for estimation of cholesteryl esters in plasma samples. See 'experimental' section for details.

## VALIDATION OF THE NEWLY DEVELOPED METHOD USING THE STANDARD INHIBITOR (AVASIMIBE)

The ACAT assay mentioned in section 2.4 was applied for the evaluation of avasimibe (known inhibitor of ACAT isoforms (Llaverias *et al*, 2003). The basic aim was to determine the $IC_{50}$ value of avasimibe for ACAT inhibition and compare it with $IC_{50}$ values determined by other methods and reported in the literature. The $IC_{50}$ value of avasimibe was found to be 4.019 ± 0.064 µM which was found to be in agreement with the value ($IC_{50}$ 4.0 µM (Burnett et al., 1999)) reported in literature. This finding indicates that the reported method can be effectively used for screening of novel ACAT inhibitors which otherwise becomes prohibitive for many researchers due to non-availability of facilities for radiometric method.

## QUANTIFICATION OF CHOLESTERYL ESTERS IN PLASMA SAMPLES

It has been reviewed that cholesteryl esters present in plasma as a part of LDL-cholesterol are responsible for the development of atherosclerosis (Spector and Haynes, 2007, Ghosh *et al*, 2010). In lieu of these reports, we chose to evaluate pathological samples having known high total plasma cholesterol levels for their cholesteryl ester content. Interestingly, a close correlation between total cholesterol levels and cholesteryl ester levels (Figure 8) was found in the present study. Previous reports have underlined a positive correlation between total cholesterol and cholesteryl esters (Zhang *et al*, 2005, Matsumura *et al*, 1999). Most of the methods employed for estimation of total cholesterol levels use cholesterol esterase to hydrolyze the cholesteryl esters (Mizoguchi *et al*, 2004). Thus cholesterol esters are indirectly estimated as a difference of total cholesterol and free cholesterol (Levy *et al*, 2007). This suggests that a significant portion of total cholesterol is derived from the hydrolysis of cholesteryl esters. It is known that the concentration of cholesteryl esters is very high in the plasma and it was customarily necessary to dilute the samples with phosphate-buffered saline before analytical measurements could be performed. Since, the curve of cholesteryl oleate is not linear at very high concentrations (>100mg/dl), results presented herewith were obtained after dilution of the samples and then multiplying the results with an appropriate dilution factor. However, care was taken to ensure that dilution patterns remained similar across all the samples of analysis so as to eliminate errors of dilution and calculation. The figure below indicates the correlation between cholesterol ester

levels and total cholesterol levels from normocholesterolemic and hypercholesterolemic individuals. The trend of the curve shows that the level cholesteryl esters are directly

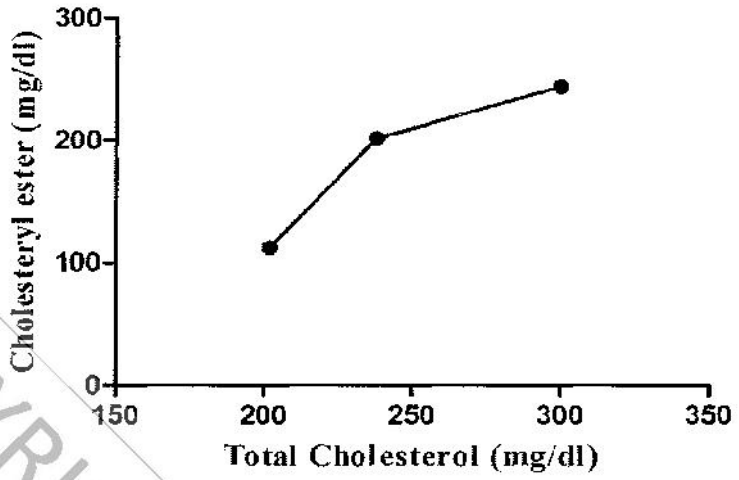


Figure 8: A plot showing the relation between total cholesterol and cholesteryl esters from plasma samples of 3 patients having total cholesterol levels higher than 200 mg/dl. Cholesteryl esters are expressed as a function of cholesteryl oleate. Results are expressed as a mean of triplicate analysis

proportional to that of total cholesterol. This finding may be in concert to that of other researchers (Spector and Haynes, 2007, Ghosh *et al*, 2010) who have suggested that cholesteryl esters may be a diagnostic factor and/or risk-marker for atherosclerosis.

**ADVANTAGES OF THE METHOD**

The method was found to have a total-run time (sample application through) of about 50-60 minutes after sample preparation hence, it can be claimed that the time of analysis is relatively short when compared to the HPLC-FLD and LC-ESI-MS/MS methods (Cao *et al*, 2013, Miyoshi *et al*, 2013). Currently, this method has been developed on a 10×10 $cm^2$ plate where 7-8 samples can be simultaneously estimated. It is also possible to use a 20×10 $cm^2$ plate where 17-18 samples can be estimated. Increasing the number of samples for analysis does not increase the time of analysis significantly as the spots are run simultaneously. The concentration range employed in the present study is 100-500 ng/band but the limit of quantification was found to be 19.54 ng/band (Table 4). Hence, this method may be applied in lower concentration ranges (i.e. 20-100 ng/band) indicating the sensitivity of this method. This sensitivity is comparable to that achieved with LC-ESI-MS/MS (30ng - 1µg; (Miyoshi *et al*, 2013). Samples and standards are estimated simultaneously on the same plate. Chances of

poisoning the sample are negligible since there is no carry over. The present method works as an open system and visual detection of the sample is possible post derivatization. Further, derivatization can be performed on the plate *in situ*. Derivatization with anisaldehyde-sulphuric acid reagent leads to the development of a purple band, so separate hydrolysis step is avoided. Using the HPTLC method, we have estimated cholesteryl esters *at par* with radiometric estimation. We were able to reproduce the data from literature regarding estimation of ACAT inhibitor avasimibe (Llaverias *et al*, 2003, Burnett *et al*, 1999). Cholesteryl ester content in plasma samples from hypercholesterolemic individuals was also estimated by this method.

## PRELIMINARY SCREENING OF TEST COMPOUNDS FOR THEIR ACAT-INHIBITION POTENTIAL

After validation of the ACAT assay and quantification of cholesteryl oleate as a product of the ACAT catalytic reaction, this method was employed for the screening of five series of urea-based novel synthetic compounds to evaluate them for their potential ACAT inhibitory activity. Since, the compounds were screened using microsomal ACAT, the activity of the compounds is represented herewith as pan-ACAT and they were not evaluated for inhibition of individual isoforms. The results of preliminary screening are depicted in the tables (8-12) below:

**Table 8: Preliminary screening of compounds from series I**

| Comps | 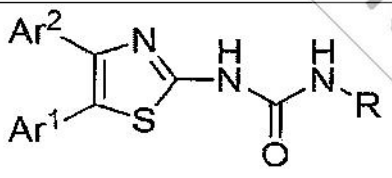 (I) | | | % Inhibition (at 10 µM conc) |
|---|---|---|---|---|
| | $Ar^1$ | $Ar^2$ | R | |
| Ia | Ph | Ph | Ph | 10.56 |
| Ib | *4*-ClPh | 4-$OCH_3$Ph | Ph | **56.86** |
| Ic | 4-ClPh | 4-$OCH_3$Ph | *n*-Butyl | 27.58 |
| Id | 4-ClPh | 4-$CH_3$Ph | *n*-Butyl | **36.37** |
| Ie | 4-ClPh | 4-FPh | 2,4-$F_2$Ph | **42.39** |

**Table 9: Preliminary screening of compounds from series II**

| Comps | 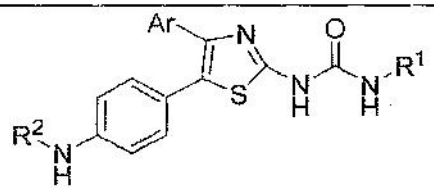 (II) | | | % Inhibition (at 10 µM conc) |
|---|---|---|---|---|
| | **Ar** | **$R^1$** | **$R^2$** | |
| IIa | 4-ClPh | 2,4-$F_2$Ph | $COCH_3$ | 2.03 |
| IIb | 4-ClPh | 2,4-$F_2$Ph | $SO_2CH_3$ | 6.39 |
| IIc | 4-ClPh | *n*-Butyl | $COCH_3$ | 3.75 |
| IId | 4-ClPh | *n*-Butyl | $SO_2CH_3$ | 5.63 |
| IIe | 4-FPh | 2,4-$F_2$Ph | $COCH_3$ | 23.32 |
| IIf | 4-FPh | 2,4-$F_2$Ph | $SO_2CH_3$ | 18.9 |
| IIg | 4-FPh | *n*-Butyl | $COCH_3$ | 15.4 |
| IIh | 4-FPh | *n*-Butyl | $SO_2CH_3$ | 0.43 |
| IIi | 4-$CH_3$Ph | 2,4-$F_2$Ph | $COCH_3$ | 3.06 |
| IIj | 4-$CH_3$Ph | 2,4-$F_2$Ph | $SO_2CH_3$ | 2.17 |
| IIk | 4-$CH_3$Ph | *n*-Butyl | $COCH_3$ | 5.23 |
| III | 4-$CH_3$Ph | *n*-Butyl | $SO_2CH_3$ | 32.67 |
| IIm | 4-$OCH_3$Ph | 2,4-$F_2$Ph | Isopropyl | **51.73** |
| IIn | 4-$OCH_3$Ph | 2,4-$F_2$Ph | *n*-Dodecyl | 1.77 |
| IIo | 4-$OCH_3$Ph | 2,4-$F_2$Ph | $COCH_3$ | **38.98** |
| IIp | 4-$OCH_3$Ph | *n*-Butyl | $COCH_3$ | **39.45** |
| IIq | 4-$OCH_3$Ph | *n*-Butyl | $SO_2CH_3$ | 5.45 |

**Table 10: Preliminary screening of compounds from series III**

| Comps | 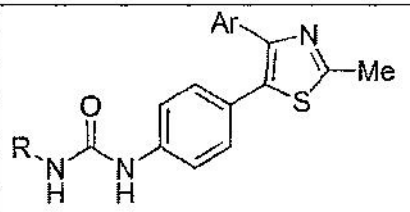 (III) | | % Inhibition (at 10 µM conc) |
|---|---|---|---|
| | **Ar** | **R** | |
| IIIa | 4-ClPh | Ph | 6.88 |

| | | | |
|---|---|---|---|
| IIIb | 4-ClPh | 2,4-$F_2$Ph | 1.3 |
| IIIc | 4-ClPh | 2,6-$(C_2H_5)_2$Ph | **63.32** |
| IIId | 4-ClPh | *n*-Butyl | **60.71** |
| IIIe | 4-ClPh | *n*-Heptyl | **52.18** |
| IIIf | 4-ClPh | *n*-Dodecyl | 5.75 |
| IIIg | 4-FPh | Ph | 16.81 |
| IIIh | 4-FPh | 2,4-$F_2$Ph | 4.97 |
| IIIi | 4-FPh | 2,6-$(C_2H_5)_2$Ph | **46.68** |
| IIIj | 4-FPh | *n*-Butyl | **59.91** |
| IIIk | 4-FPh | *n*-Heptyl | **62.96** |
| IIIl | 4-FPh | *n*-Dodecyl | 34.47 |
| IIIm | 4-$CH_3$Ph | 2,6-$(C_2H_5)_2$Ph | 30.94 |
| IIIn | 4-$CH_3$Ph | *n*-Butyl | **64.91** |
| IIIo | 4-$CH_3$Ph | *n*-Heptyl | 33.41 |
| IIIp | 4-$CH_3$Ph | *n*-Dodecyl | **46.19** |
| IIIq | 4-$OCH_3$Ph | Ph | 11.37 |
| IIIr | 4-$OCH_3$Ph | 2,4-$F_2$Ph | 22.27 |
| IIIs | 4-$OCH_3$Ph | 2,6-$(C_2H_5)_2$Ph | 31.62 |
| IIIt | 4-$OCH_3$Ph | *n*-Butyl | **40.02** |
| IIIu | 4-$OCH_3$Ph | *n*-Heptyl | 22.21 |

**Table 11: Preliminary screening of compounds from series IV**

| **Comps** | 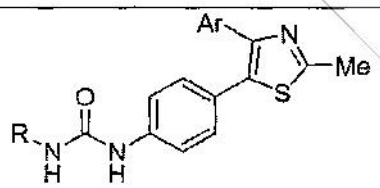 **(IV)** | | **% Inhibition (at 10 µM conc)** |
|---|---|---|---|
| | **Ar** | **R** | |
| IVa | 4-ClPh | 3,4,5-$(OCH_3)_3$Ph | 24.44 |
| IVb | 4-ClPh | 2,6-$[CH(CH_3)_2]_2$Ph | 12.64 |
| IVc | 4-ClPh | Morpholinoethyl | 12.31 |
| IVd | 4-FPh | 3,4,5-$(OCH_3)_3$Ph | **41.98** |
| IVe | 4-FPh | 2,6-(*iso*-propyl)$_2$Ph | **42.12** |
| IVf | 4-$CH_3$Ph | 3,4,5-$(OCH_3)_3$Ph | 21.88 |

| | | | |
|---|---|---|---|
| IVg | 4-$CH_3$Ph | 2,6-(*iso*-propyl)$_2$Ph | 11.19 |
| IVh | 4-$OCH_3$Ph | 3,4,5-$(OCH_3)_3$Ph | 25.44 |
| IVi | 4-$OCH_3$Ph | 2,6-(*iso*-propyl)$_2$Ph | 30.13 |
| IVj | 4-$OCH_3$Ph | Morpholinoethyl | 21.46 |

**Table 12: Preliminary screening of compounds from series V**

| Comps | 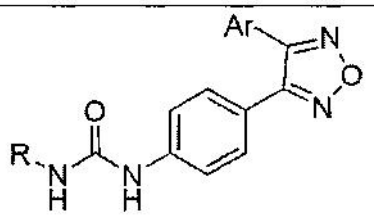 (V) | | % Inhibition (at 10 µM conc) |
|---|---|---|---|
| | Ar | R | |
| Va | 4-ClPh | 2,4-$F_2$Ph | 21.23 |
| Vb | 4-ClPh | 2,6-$(C_2H_5)_2$Ph | 8.25 |
| Vc | 4-ClPh | *n*-Butyl | 23.03 |
| Vd | 4-ClPh | *n*-Heptyl | 4.3 |
| Ve | 4-ClPh | *n*-Dodecyl | 18.51 |
| Vf | 4-FPh | 2,4-$F_2$Ph | **47.06** |
| Vg | 4-FPh | 2,6-$(C_2H_5)_2$Ph | **44.85** |
| Vh | 4-FPh | *n*-Butyl | **54.5** |
| Vi | 4-FPh | *n*-Heptyl | 30.93 |
| Vj | 4-FPh | *n*-Dodecyl | **50.7** |
| Vk | 4-$CH_3$Ph | 2,4-$F_2$Ph | 13.52 |
| Vl | 4-$CH_3$Ph | 2,6-$(C_2H_5)_2$Ph | 0.34 |
| Vm | 4-$CH_3$Ph | *n*-Butyl | 2.83 |
| Vn | 4-$CH_3$Ph | *n*-Heptyl | 18.65 |
| Vo | 4-$CH_3$Ph | *n*-Dodecyl | 9.15 |



Based on the preliminary screening data, it was observed that several compounds showed good inhibition (some of them ≥ 60%) which was comparable to that of known pan-ACAT inhibitor avasimibe. This data was used further to select compounds for determination of $IC_{50}$. A threshold value of 35% inhibition was arbitrarily selected and all those compounds showing ≥ 35% inhibition of microsomal

ACAT activity were selected for $IC_{50}$ determination at five different concentrations. The execution of $IC_{50}$ determination was identical to that of the preliminary screening except that five non-zero concentrations were used to determine ACAT-inhibition potential for each compound. The results are shown below (Table 13):

**Table 13: Determination of $IC_{50}$ on ACAT for selected compounds**

| Comps | $IC_{50}$ (µM) | Comps | $IC_{50}$ (µM) |
|---|---|---|---|
| Ib | 10.66 ± 1.02 | IIIj | 9.58 ± 0.81 |
| Id | 93.95 ± 1.97 | IIIk | **5.69 ± 0.75** |
| Ie | 18.37 ± 1.26 | IIIl | 46.83 ± 1.67 |
| IIm | 12.11 ± 1.08 | IIIn | **2.43 ± 0.38** |
| IIo | 31.86 ± 0.71 | IIIp | 12.18 ± 1.08 |
| IIp | 41.29 ± 0.58 | IVd | 12.62 ± 0.82 |
| IIIc | **4.04 ± 0.60** | IVe | 11.84 ± 0.84 |
| IIId | **6.27 ± 0.80** | Vf | 20.09 ± 1.30 |
| IIIe | **7.85 ± 0.89** | Vg | 9.73 ± 0.98 |
| IIIi | **8.40 ± 0.92** | Vj | 12.44 ± 1.09 |



Table 13 shows that the $IC_{50}$ values of several compounds (IIIc, IIId, IIIe, IIIi, IIIk, and IIIn) are well below 10 µM. Several urea based compounds available in the literature are known to show good inhibition of microsomal ACAT activity. These compounds are usually tri- or di-substituted derivatives of urea with myriad of substituents on either side. All of the series listed above involve di-substituted derivatives of urea. Several researchers have reported individual SAR studies with their own di-substituted urea derivatives which have shown promise for ACAT-inhibition *in vitro* and good anti-hypercholesterolemic activity. These compounds were found to exhibit microsomal ACAT-inhibition in the $IC_{50}$ range of 0.007-5.300 µM (Kimura *et al*, 1993; Kumazawa *et al*, 1995; Trivedi *et al*, 1995; Gelain *et al*, 2006; Asano *et al*, 2009). These activities may seem promising and comparable to the standard inhibitors of ACAT like avasimibe and pactimibe but some of these compounds had their inherent problems like low water solubility, low absorption through the GIT, adrenal toxicity and complexity of synthetic process which led to retraction in their pursual (Kimura *et al*, 1993; Dominick *et al*, 1993a; 1993b; Tawada *et al*, 1994; Trivedi *et al*, 1995).

Change in substituents, inclusion of heteroaryl moieties and hydrohphilic groups were tried to improve the overall pharmacological acceptability of these compounds. Similar approaches were carried out in the synthetic series used for the present study to generate a range of novel compounds which could show potent inhibition of ACAT. As is evident from the results, compounds of series III have shown good inhibition of microsomal ACAT. So far, compound **IIIn** was found to be the most potent inhibitor of microsomal ACAT *in vitro*. The *in vitro* data for **IIIn** is comparable to that reported for avasimibe (Llaverias et al, 2003). These active compounds were further evaluated in a model of triglyceride turnover.

**POLOXAMER-407 INDUCED LIPOPROTEIN LIPASE INHIBITION MODEL**

Triglycerides are water insoluble molecules that are considered to be rich sources of energy for extrahepatic tissues. They are secreted from the liver as subsets of VLDL particles. It has been observed that overproduction of VLDL leads to a direct disposition of an individual towards CHD. Increase in triglyceride production rates have been observed after inhibition of plasma lipoprotein lipase (responsible for TG hydrolysis) and thereafter observing the temporal changes in plasma TG levels (Johnston and Palmer, 1993; Chang *et al*, 2006a; Temel *et al*, 2007). Several studies have utilized Triton WR-1339 (*tyloxapol*®) for inhibition of lipoprotein lipase where TG production rate was calculated over time after Triton WR-1339 injection (Erickson *et al*, 1980a; Aragane *et al*, 1998). However, it has been observed that there are several possible variables which may induce errors in the results (Millar *et al*, 2005). These variables include fasting/fed conditions, fat-free diet, plasma sampling period, plasma holding time and methods of TG analysis over linearity curves. However, these variables can be controlled at the experimenter's discretion but there are few physiological effects related to Triton WR-1339 which might suggest that an alternative agent may be used. These effects include dissociation of ApoA-I and ApoC-II from HDL particles, accumulation into lysosomes and causing formation of autophagic vacuoles, secretion in bile and excretion *via* the liver which might point towards a reduction in biliary cholesterol output and most importantly a gradual decline in TG production rate after the first hour making it difficult to interpret data after 3-4 hours. Alternatively, Poloxamer-407 or P-407 (*Pluronic*® *F-125*) a non-ionic detergent also inhibits lipoprotein lipase. Initially it was used as a co-polymer for controlled drug

delivery but was later found to be an inhibitor of lipoprotein lipase. The advantages of P-407 over Triton WR-1339 are (Millar *et al*, 2005):

1. Flexibility in sampling with same production rates
2. Study can be extended upto 48-72 hrs
3. Dissolution of HDL particles is not an issue
4. Preferential renal excretion owing to the HLB difference
5. No accumulation in lysosomes so TG trafficking remains unaffected
6. Hepatic lipid production is not affected

Figure 9 shows the effects of different compounds on triglyceride (TG) turnover following P-407 administration. It indicates that, commensurate with the *in vitro* data, compound **IIIn** is also active *in vivo*. The effect of **IIIn** is evident from the fact that the **IIIn** administered group shows only moderate changes in TG turnover (~20 fold) over a period of 24 hrs. Similar effect was also observed in the avasimibe group. While control animals showed a mean 80-fold change in baseline TG levels, other

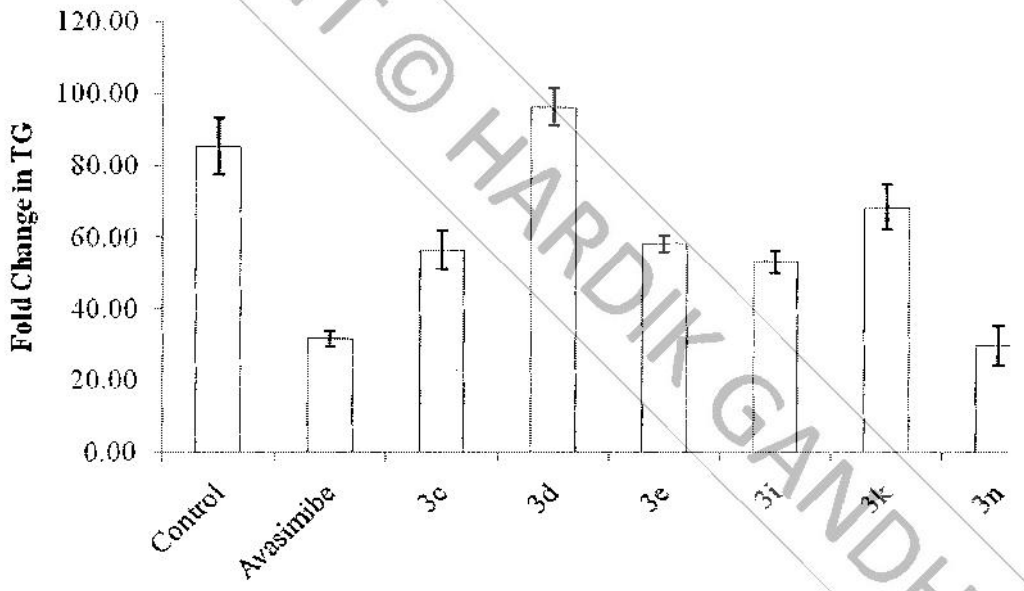


Figure 9: effects of P-407 on 24 hr triglyceride turnover measured as fold-change in TG at 0 hr and 24 hr after administration of P-407.

groups showed 50-90 fold changes in TG turnover which was exceedingly high in comparison to the standard and **IIIn** group. Since this study has already established that **IIIn** is a pan-ACAT inhibitor, it was interesting to identify the effects of this compound on TG turnover. However, these findings stand in stark contrast to those reported by Erickson *et al*, (1980b) who showed that administration of triton WR 1339 showed modest reduction in ACAT activity by itself and ACAT-inhibition, *per se*, has no effect

on lipid turnover. On the other hand Aragane *et al*, (1998) and Uchida *et al*, (1998) reported that known inhibitors of ACAT prevent the cholesteryl-ester input in plasma and reduce hepatic TG secretion rate. The present experiment revealed that there might be correlation between ACAT inhibition and TG turnover since avasimibe was also active against TG turnover mediated through LPL inhibition. It is known that chylomicrons (which form the significant chunk of TG), after losing triacylglycerols acquire cholesteryl esters from other lipoproteins. Since administration of ACAT-inhibitors can prevent *de novo* formation of cholesteryl esters, the pool of cholesteryl esters that remains available for acquisition by chylomicrons is depleted. This biochemical inhibition thus correlates with the observations of the present study where administration of ACAT inhibitors like avasimibe and the test compound **IIIn** resulted in a reduced TG turnover *in vivo*. Based on the results, it was decided to evaluate compound **IIIn** in a model of athersoclerosis since compound **IIIn**, apart from microsomal ACAT inhibition, also showed favourable effect on serum lipids.

Henceforth, compound **IIIn will be encoded as MCR-788** as per laboratory norms.



## TOXICOLOGICAL EVALUATION OF MCR-788

### *Single dose acute oral toxicity*

Studies with different urea-based derivatives belonging to this class of compounds have not shown any fatal toxicity signs. These studies have reported a safety of assorted urea-derivatives upto 2000 mg/kg and beyond (Lee *et al*, 2013; Robertson *et al*, 2000). Some compounds were reported to exhibit adrenal toxicity at high doses which may be an indication of non-specific cytotoxicity rather than their ACAT-inhibition potential (Dominick *et al*, 1993a; Roth, 1998). To ensure the safety of the test compound, **MCR-788** was administered at the recommended dose. The post-treatment examination period was 14 days from the date of dosing. Body weights of the animals were recorded on days 0, 7 and 14. Slight fluctuations were observed in the body weight of animals but since they were within 20% of the mean body weight no additional measurements were taken and any other precaution was not followed. The animals were closely observed during the first 6 hours after dosing. The animals were starved during this period with access to water. No significant observations were recorded during this period. This part coincided with the light cycle and most of the

time animals were asleep. When awake, the animals showed normal grooming behavior and water intake was also normal. During the entire post-treatment observation period special attention was paid to alteration of skin or fur, abnormal locomotion or breathing and changes in the eye. No untoward observations were made in this regard until the terminal day of the study. Mortality was recorded twice daily but no mortality was found in any dose group until day 14. At the end of the study period, the animals were euthanized and major organs (brain, heart, lung, liver, kidney, spleen and adrenals) were harvested. Gross necropsy was performed by an individual blinded to the groups. No macroscopic lesions were recorded. Viscera, gastrointestinal tract and mucous linings appeared normal. Adrenal glands exhibited normal size & shape and any signs of shrinkage were absent. Detailed report on toxicity evaluation is presented as Appendix III.

Administration of 2000 mg/kg of **MCR-788** showed no signs of toxicity or mortality during the test period. The $LD_{50}$ of **MCR-788** in rats was thus found to be >2000mg/kg.

***Repeat dose oral toxicity***

At the end of the study, no untoward observations were made regarding body weight, food intake or normal behavior. Gross necropsy did not reveal any suggestive lesions or abnormal anatomical feature. Adrenal glands appeared normal. The most plausible side effect related to the mechanism of action of **MCR-788**, upon repeat-dose administration, could be cutaneous xanthomatosis (Yagyu *et al*, 2000; Farese, 2006; Ohshiro *et al*, 2011). This effect was not evident in any subject of the study even at the extended 14-day period. Biochemical estimations did not suggest any major digression from normal values. Urinary output and hematological data appeared normal. Urea based compounds promoted as ACAT inhibitors have been known to be safe at doses upto 60 mg/kg or less. Detailed report on repeat dose toxicity evaluation is presented as Appendix IV.

It was concluded that chronic administration of **MCR-788** at a dose level of 60mg/kg was safe.

## EVALUATION OF MCR-788 IN A MODEL OF DIET-INDUCED ATHEROGENESIS

A model of diet-induced atherogenesis has been reported to be a valid model for study of compounds expected to be effective against atherosclerosis.

***Significance of ingredients in the atherogenic diet***

Cholesterol and coconut oil provide the caloric intake in the form of fat calories and thus carbohydrate calories are reduced. It has been studied that casein promotes casomorphin- or peroxidase-dependent oxidation of LDL through generation of tyrosyl free radicals (Kritchevsky, 1995; Tailford *et al*, 2003). Additionally, it may also promote atherogenesis by causing endothelial dysfunction mediated through invasion of the endothelia by monocyte/macrophages (Tailford *et al*, 2003; Matsuzawa *et al*, 2007). Cholic acid helps in the absorption of cholesterol through micellar solubilisation (Nishina *et al*, 1990; Vergnes *et al*, 2003). This property prevents the excretion of excess cholesterol taken in the form of diet and helps in the development of hypercholesterolemia. However, wistar rats are very robust and have high HDL-C and low LDL-C concentrations in plasma. It is very difficult to induce atherosclerosis in such wild-type animals without the inclusion of 2-thiouracil. 2-Thiouracil is a thyroid hormone inhibitor which prevents thyroid hormones from reducing elevated LDL-C, triglycerides, cholesterol and lipoprotein a [Lp(a)] (Joris *et al*, 1983). All these changes prompt the development of atherogenic lesions.

***Body weight***

The curve of body weight remained relatively unaffected for all the groups. No significant change in body weight was observed between the final and initial stages of the study. At the end of the study there was no significant difference between the progression control group (290.3 ± 8.1 g), **MCR-788** (10 mg/kg) treated group (294 ± 14.3g) and **MCR-788** (30 mg/kg) treated group (299 ± 6.6 g). Previous studies on similar lines have also reported that body weight remains comparable in all the groups (Maechler *et al*, 1992; Kusunoki *et al*, 2001; Ohshiro *et al*, 2011). Figure 10 shows the difference in body weights among the groups.

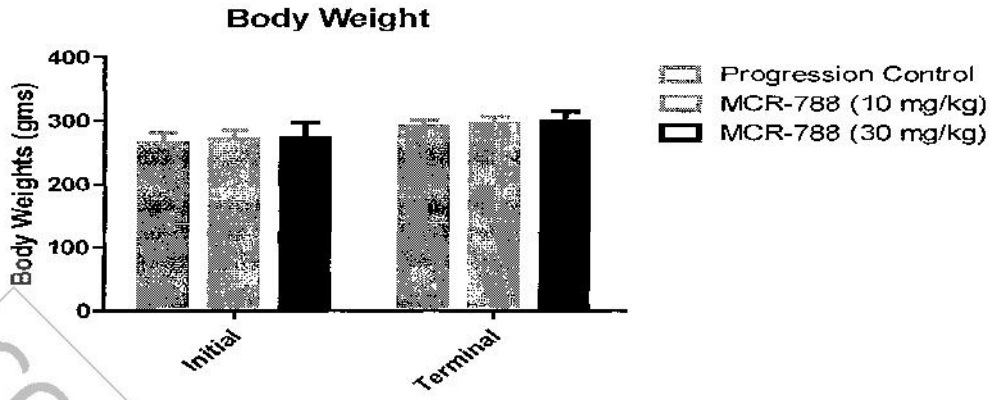


Figure 10: Figure shows mean body weight of all the groups before and after treatment. It may be noted that no significant change was observed between any groups towards the end of the study.

***Analysis of serum lipids and lipoproteins***

Effects of atherogenic diet and treatment with **MCR-788** on lipid profile are depicted in figure 11. At the initiation of the study the mean cholesterol values for all the animals averaged around 91.16 ± 4.54 g. It was observed that cholesterol levels start rising dramatically after about 2-weeks of HCD initiation and keep rising towards the terminal stage of the study in the progression control group. These findings are similar to those reported by other groups utilizing similar models for development of atherosclerosis (Maechler *et al*, 1992; Kusunoki *et al*, 2001). A dose-dependent prevention of serum total cholesterol elevation was observed in the groups (Figure 11A) that were co-administered **MCR-788**. The effect of 10mg/kg in preventing cholesterol elevation was not found to be significant but the 30 mg/kg dose-group showed drastic prevention of cholesterol elevation with serum total cholesterol levels being 138 ± 9.50 g at the end of the study. On the contrary, as expected HDL-C values showed a downward trend as the study progressed and a 2-fold reduction in serum HDL-C levels was observed in the control group. Such changes are similar to the reduced HDL-C levels reported by other groups (Maechler *et al*, 1992) Treatment with **MCR-788** was able to show a dose-dependent prevention of HDL-C reduction (Figure 11B). Minor elevations in triglyceride levels between the initial and final stages of the study were observed but were not found to be statistically significant (*P* value 0.251; Figure 11C). Analysis of lipoprotein cholesterol levels, LDL-C and VLDL-C, were based on the Friedewald's formula and showed that VLDL-C elevations were not significant among the groups (Figure 11D). However, a sharp rise in LDL-C (more than 12-fold) was observed in the progression control group ($P<0.001$). The lower dose group showed

only modest prevention in LDL-C elevation but the **MCR-788** 30 mg/kg dose group indicated a significant prevention ($P<0.001$; Figure 11E) of LDL-C elevation as compared to the progression control group. Based on these data, the atherogenic index was calculated, which indicates the prevalence of non-HDL cholesterol over HDL-C. This data indicated that after 8 weeks of HCD administration the atherogenic index peaks to 19.59 ± 5.8. Such a high value of the atherogenic index indicates that the animals were prone to the development of atherosclerotic lesions. Co-administration of **MCR-788** in the diet reduced the atherogenic index to 7.55 ± 0.9 and 1.82 ± 0.34 respectively in the 10 mg/kg and 30 mg/kg groups (Figure 11F).

Different disubstituted urea-based ACAT inhibitors reported in the literature have shown good cholesterol lowering properties *in vivo* (Kimura *et al*, 1993; Reindel *et al*, 1994; Gelain *et al*, 2006). It has been shown that these derivatives exhibit excellent efficacies for development as anti-atherosclerotic agents. These compounds not only improve total cholesterol levels but also increase the HDL-C titre which might be related to their protective effects. White *et al*, (1996) and Ohnuma *et al*, (2004) have reported substituted ureas as potent agents which improve triglyceride and cholesterol levels in plasma and have shown efficacy comparable to that of atorvastatin, the drug of choice in atherosclerosis. The animal models utilized in these studies were rats, mice, rabbits or genetically modified mice but the results shown by them indicated that these urea-derivatives showed potent inhibition of ACAT, *in vivo*, culminating in atheroprotection. Hence, the beneficial effect of **MCR-788** in similar conditions may be anticipated in light of the data presented above.

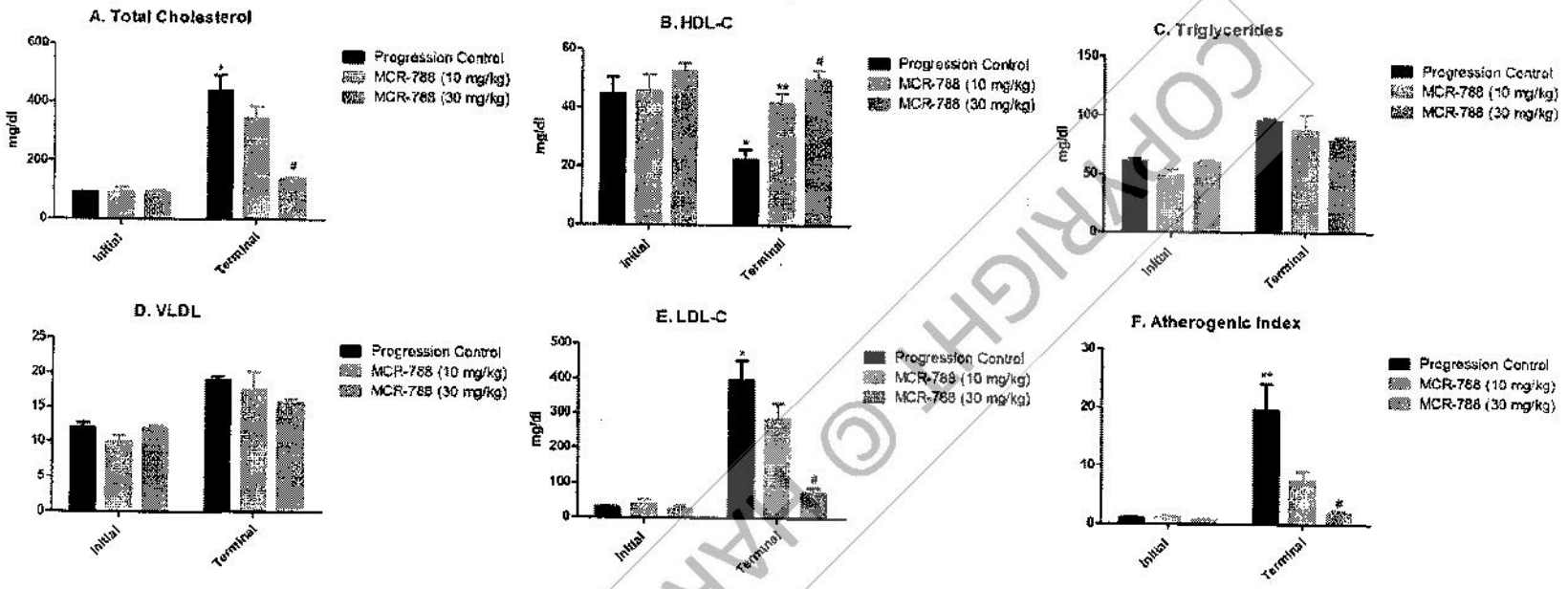


Figure 11: Figures represent the lipid profile of all the groups at the initial and terminal phases of study. A, Total cholesterol levels are increased in the progression control group at the end of 8 weeks. Significant prevention of cholesterol elevation is observed in the **MCR-788** high-dose treated group. B, Pathological development of hypercholesterolemia has led to significant reduction in the levels of HDL-C. Such abnormalities are not observed with the treated animals. C, No major fluctuation in the triglyceride levels was observed between groups. D, Since VLDL-C values were derived from triglyceride levels, the results were expected to be similar. E, Friedewald's equation revealed that LDL-C was significantly elevated in the progression control group. Treatment with low dose **MCR-788** showed only modest effect but high-dose **MCR-788** led to a significant prevention in elevation of LDL-C levels and were found to be similar to those at the beginning of the study. F. Atherogenic index was very high in the progression control group as compared to the treatment group indicating the protective effect of **MCR-788**. For all the observations, '*' indicates $P<0.05$ as compared to initial data at Day 0; '**' indicates $P<0.01$ as compared to initial data at Day 0 or as compared to the progression control group at 8 weeks; '#' indicates $P<0.01$ as compared to the progression control group at 8 weeks.

***Lipid accumulation lesion area in the aortae***

Lesion area in the aortic strips were characterized by *en face* lipid staining with Sudan red IV. Photographs of pinned aortae (Figure 12) upon area analysis by ImageJ revealed that 22.35±7.9 % area from the progression control group was stained as compared to the 16.21±1.07% ($P>0.05$) in the 10 mg/kg groups and 8.42±2.7% ($P<0.05$) in the 30 mg/kg group. Several studies have identified the potential of ACAT inhibition in reducing the lesion area. Ohshiro *et al*, (2011) represented a dose-dependent effect of ACAT-inhibition on lesion development while the results of Kusunoki *et al*, (2001) showed that F-1394 (a pan-ACAT inhibitor) prevented the development of atherosclerotic lesion to more than 40%. Chiwata *et al*, (2001) also showed dose-dependent protective effects of F-1394 on atherosclerotic lesion development. Results of the present study indicated that treatment with 30 mg/kg **MCR-788** shows nearly 3-fold reduction in the lesion area as compared to the progression control (Figure 13).

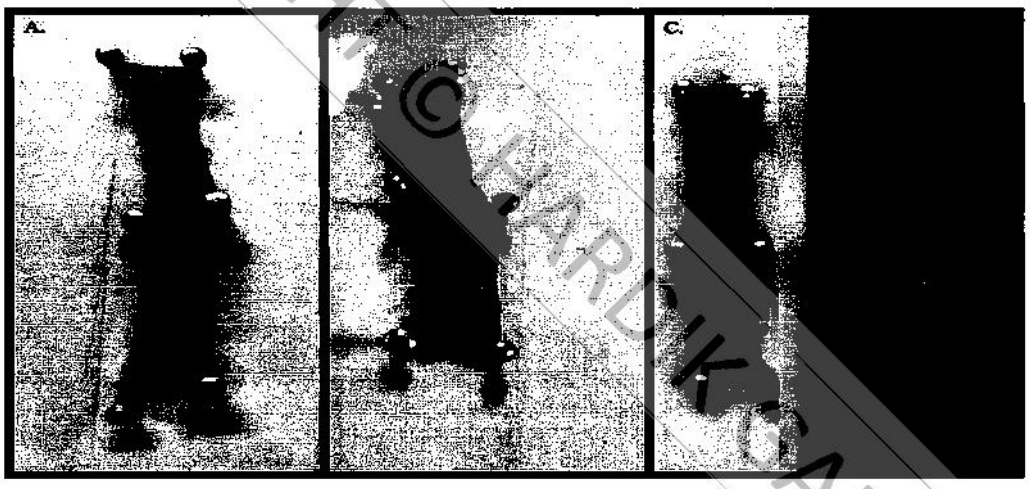


Figure 12: This figure shows representative aortae from each group. A, Accumulation of lipids in the intimal area result in the formation of fatty streaks which are stained maroon in color in the progression control group. This type of streaks are evident along the length of the aorta. B, The 10 mg/kg group also shows such intermittent streaks but as it is evident from the photograph, deposition has been minimised to a reasonable extent and C, Absence of any fatty streaks can be observed in this image. This is indicative of the atheroprotective role of **MCR-788** (30 mg/kg).

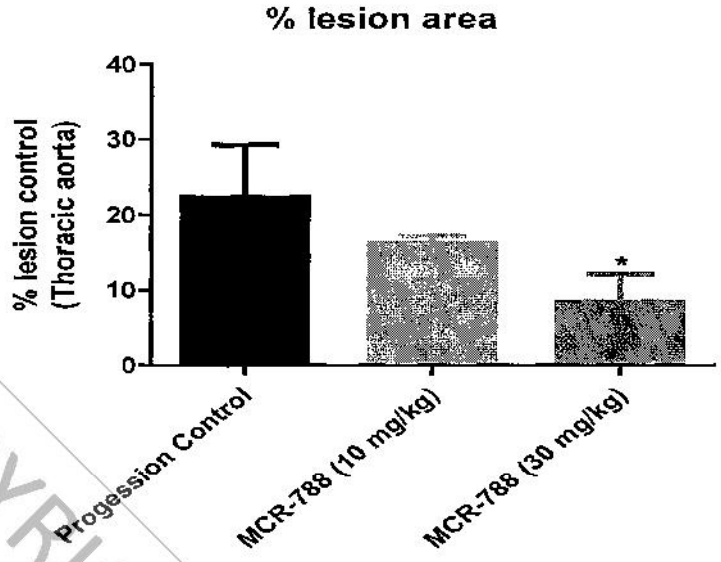


Figure 13: Fatty streaks observed by *en face* lipid staining were analysed by the ImageJ image analysis software and the lesion areas (stained maroon) were calculated respective to the total aortic strip area. Data are presented in the figure as mean ± SEM of lesion area. It can be observed that 30 mg/kg of **MCR-788** resulted in a significant prevention of lesion development. '*' indicates $P<0.05$ as compared to the progression control group at the end of 8 weeks.

***Lumenal lipid plaque identification***

Lumenal plaque formation was studied by taking multiple sections of the aortae and then staining them with Sudan Red IV to stain the lipid core of the plaque. Cryosections were used for the present study since conventional paraffin-block sectioning and deparaffinization methods utilize organic solvents which can crucially affect lipid content in the plaque core and give false-negative results. Since cryosectioning methods are solvent-free, they are recommended for such studies where solvents might affect the results. The sections were stained with Sudan Red IV to visualize the lumenal lipids.

Representative images from different groups are shown in the figure 14. The figures indicate that long-term consumption of an atherogenic diet has led to development of a plaque core which has obscured the lumen of the aortic root (*a.k.a.* aortic sinus). Aortic root is the most putative site for formation of lipid-rich plaques, although a plaque may be formed in any anatomical region of the artery. Such observations have been reported by Ohshiro *et al*, (2011) who have shown thickened intima in progression control groups. Other researchers like Kusunoki and colleagues (2001) suggest typical lesions in the aortic root cross sections and prevention of such lesions following ACAT-inhibitor therapy. Namatame *et al*, (2004)

also showed development of proximal root lesions following a high-cholesterol diet and its prevention with fungal ACAT-inhbitors (beauverolides). No evidence for the development of lipid-rich cores was found in animals treated with **MCR-788** in the present study.

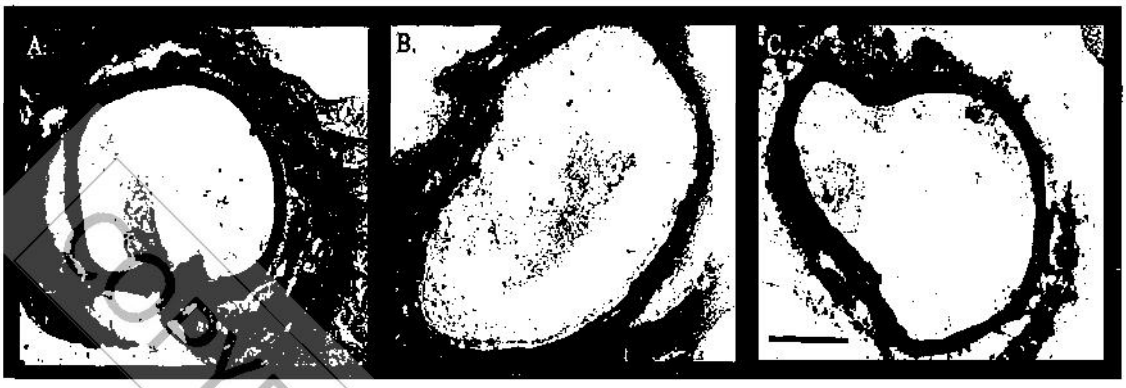


Figure 14: This figure represents the cross-sectional areas from aortic roots after sacrificing animals of the different groups. Streaks in the intimal area are not observed in any group but development of plaque is evident in the HCD progression control (A). Minor damage to the arterial wall is evident at the region where plaque development is initiated. Intimal linings appear normal and there is no evidence of diameter obscuration in the treated groups (B and C). The scale bar in figure C represents 500 μm.

It was notable that protective effects of **MCR-788** reported in the study were obtained without any evidence of cutaneous or adrenal toxicities. In contrast, the study revealed that **MCR-788** was not only safe but also effective in reducing the biochemical profile and lesions in an atherogenic model. Based on this study, the potential of this compound as a lead candidate against atherosclerotic disease cannot be denied.